Forecasting Crude Oil Returns using News Sentiment and Machine Learning *

Tianyu Du †

Saturday 18th April, 2020

Contents

*Compile Date: 21:01 Saturday 18th April, 2020

†tianyu.du@mail.utoronto.ca

1 Introduction

Algorithmic trading systems are playing a significant role in nowadays financial markets. Strategies in most of these trading systems are based on predictive models: one asset is sold (bought) if the model predicts its prices is going to fall (rise). Therefore, profitabilities of algorithmic trading systems highly depend on predictive models. This paper focuses on the crude oil market since crude oil prices not only serve as investing instrument but also an important predictor of other economic indicators. Studying whether it is possible to build new predictive models and improve current models is relevant to both investors and economists.

The contribution of this paper to current literature is three-fold:

- This paper examines whether the crude oil market is predictable (efficient) with respect to historical crude oil price/return movements and sentiments of news related to crude oils.

- With the series of crude oil returns from Energy Information Administration (EIA) and the dataset of news sentiments from Ravenpack News Analytics (RPNA), this paper constructs a return series from spot prices of crude oil and identifies the day-of-the-week effect in crude oil returns. The autocorrelation function and partial autocorrelation function suggest that the intertemporal correlation with return series is weak, therefore, future returns are essentially unpredictable using historical returns only. Results of Kolmogorov-Smirnov test suggest that the empirical distribution of Mondays' returns are significantly different from distributions of returns on other days of the week. Last but not least, this paper constructs a multivariate time series of news sentiments from individual news articles, such series allows machine learning models to predict returns based on news sentiment simply by including more independent variables.

- Lastly, this paper proposes a framework for forecasting crude oil returns using news sentiments. Using this framework, experiment results suggest incorporating news sentiments does make crude oil returns more predictable but this is not true for all classes of models

There are three major benchmarks for crude oil price: West Texas Intermediate (WTI), Brent Crude and Dubai/Oman and they measure tradings of crude oils produced in the U.S., Europe, and the Middle East respectively. Mann and Sephton (2016) examine the relationship between these three crude oil price benchmarks and indicate that these benchmark prices are tied by a long-run relationship. Moreover, their analysis shows that all three benchmarks are moving to restore the observed long-run relationship in at least one regime (Mann and Sephton 2016). Therefore, the same predictive model should achieve similar performances on three markets at least in the long run, and conclusions drawn on one market can be extended to the other two markets. Because the news sentiment dataset used in this paper consists of news published by four U.S. based publishers, this paper focuses on the WTI crude oil spot price among all three main crude oil benchmarks. Instead of predicting the spot price of crude oil, I am going to forecast the series of empirical returns since returns can better reflect the profitability. This paper aims to answer the following research questions:

Whether the daily return of crude oil is predictable or not? Can we better predict returns by incorporating news sentiments?

In particular, this paper aims to examine the feasibility of predicting the empirical return on crude oil the next day based on information up to the current day.

Research questions can be answered by testing different versions of the **efficient market hypothesis** (EMH) (Fama 1970, Fama 1991). Jensen (1978) provides a minimal definition of the EMH and defines a market to be efficient with respect to an information set Ω if it is not profitable to trade solely using this information set. The strength of one particular version of EMH depends on the content of Ω in its definition. For convenience, this paper defines the following two information sets:

- Ω_{partial}: the information set containing historical returns only,
- Ω_{complete}: the information set consisting of both historical returns and news sentiment.

The weakest version of EMH consists of a Ω_{partial} as its information set and suggests that any trading strategy using a forecaster based on historical price movement would only generate zero (expected) economic profit. Equivalently, the weak EMH of the crude oil

market holds if the crude oil market is unpredictable by models using historical returns only.

Similarly, this paper uses $\Omega_{complete}$ to define the stronger EMH, which suggests the current crude oil market has already absorbed and reflected all price movements and news. Empirically, the stronger EMH suggests that a trading strategy built upon predictive models using both historical returns and news will not generate positive (expected) economic profit. Equivalently, the stronger EMH of the crude oil market says the crude oil returns are unpredictable even using models that incorporate both historical returns and news sentiment.

Timmermann and Granger (2004) review the concept of EMH in the context of forecasting and extend Jensen's definition to include types of predictive models (called model class) and model selection method (termed search technology):

A market is efficient with respect to the information set, search technologies, and the class of predictive models if it is impossible to make economic profits by trading on the basis of signals produced from a predictive model defined over predictor variables constructed from the information set and selected using the search technology (Timmermann and Granger 2004).

I select best models from various classes of machine learning models such as random forests, support vector machines and deep neural networks using randomized cross-validation techniques (search technology).

For each information set, the corresponding EMH can be tested by comparing the test time performances of models mentioned above and other benchmark predictors. For instance, the best random forest model identified using a given searching technology and trained using Ω_{partial} can only achieve similar accuracies compared with another native predictor, which predicts zero returns all the time, then I can conclude the market to be efficient with respect to the partial information set, random forests and randomized cross validation.

Because contents of Ω_{partial}, predictive models and the search technology in this paper are all publicly available, the predictive power of models trained on the partial information should be self-destructive: as more traders find this predictive power, they will trade accordingly and this advantage eventually vanishes (Timmermann and Granger 2004). This paper looks into the 20 year period from 2000 to 2019, we do not expect predictive powers (if any) of models based on publicly available information to be persistent over 20 years. Therefore, we expect the crude oil market to be efficient on the partial information set.

Given the class of predictive models trained and search technology used, I am going to examine both the weak EMS with Ω_{partial} and the strong EMH defined by Ω_{complete}. This paper could (i) conclude the market is unpredictable using information, models and searching technologies in this paper and (ii) news sentiments do not help predict crude oil returns.

In contrast, if the weak EMH holds but strong version fails, this servers as an evidence suggesting (i) the crude oil market is predictable and (ii) incorporating news sentiments helps predict returns.

Subsequent sections of this thesis consist of the following parts: literature review, data analysis, framework, experiments, and conclusion. The literature review section provides a brief review of current time series forecasting methodologies and research on forecasting crude oil prices/returns. In the data analysis section, we construct an empirical return of crude oil from the series of spot prices. In addition, this paper analyzes the return series and news sentiment datasets in detail. Then, this paper proposes a structured model capturing the interdependencies among states of the world, crude oil return series, and flow of news. Using the proposed framework, this paper formulates the forecasting problem into a generic supervised learning problem that fits into a vast majority of existing machine learning models. We then test our null hypothesis by comparing the performances of different models under the proposed framework. Lastly, we conclude our findings and discuss the limitations and potential improvements.

2 Literature Review

Traditional time series methods explore endogenous patterns encoded in the series of returns and use lagged values of returns to forecast future returns. Mohammadi and Su examine the performance of autoregression integrated moving average-generalized autoregressive conditional heteroskedasticity (ARIMA-GARCH) on eleven international crude oil market. The authors apply ARIMA-GARCH models to forecast the value and volatility of weekly crude oil returns in those markets and conclude that the return is characterized by a MA(1) process (Mohammadi and Su 2010).

In addition to using historical returns as features, many are utilizing other technical indi-

cators of the market as well. These methods aim to transform lagged values of return into meaningful predictors such as moving averages (MA) and moving average divergence convergence (MADC). Baker and Wurgler construct an investor sentiment index for the stock market using a collection of technical indicators: the closed-end fund discount, NYSE share turnover, numbers of IPOs, average first-day returns, and share of equity issues in total equity and debt issues, dividend premium (BAKER and WURGLER 2006). Moreover, a more recent study constructs market sentiment indices for both WTI and Brent oil future markets, and these constructed indices have shown significant predictive power while controlling external variables such as stock indices and exchange rates (Deeney et al. 2015).

More recently, besides exploring the predictive power of market indices, scholars are paying more attention to alternative data sources such as news. The inceptions of most market partitioners are in fact shaped by what news they have heard, and these partitioners trade commodities, stocks, and other financial derivatives based on news they receive. In Bybee and others' recent work, they analyze the full-text contents of over 800,000 articles on the Wall Street Journal over the past 30 years. They have demonstrated that text-based features from news articles can track economic activities accurately. Moreover, these text-based features have additional predictive powers to traditional macroeconomic indicators for macroeconomic forecasting (Bybee et al. 2019). Most works exploring and utilizing the predictive power of news sentiments are focusing on the stock market. Tetlock analyzes the interaction between articles in the "Abreast of the Market" column in the Wall Street Journal and the stock market. Using vector autoregression (VAR), Tetlock models the intertemporal correlation between the stock market and a measure of media pessimism constructed using principal component analysis (PCA). The author finds pessimistic signals in news media can a precursor of downward pressure on stock price and high trading volume (Tetlock 2007). Mudinas, Zhang, and Levene demonstrate that news sentiments extracted from Financial Times and tweets Granger cause prices of several stocks in S&P500. Experiments in their paper suggest the prediction accuracies of support vector machines and recurrent neural networks are improved by utilizing additional news sentiment features (2019). Hu and others designed a Hybrid Attention Network (HAN) to extract information and forecast price movements. Beyond accurately predicting trends in the stock market, trading algorithms based

on the proposed predictive model demonstrate superior annualized return in the Chinese stock market compared with other algorithms (Hu et al. 2018).

Instead of the stock market, Roache and Rossi analyze the impacts of macroeconomic announcements on daily prices of 12 commodity futures including oil, heating oil and natural gas between 1997 and 2009. Their experiments show that commodities are in general insensitive to macroeconomic news and models based on news perform poorly on forecasting daily prices of commodities (Roache and Rossi 2010). Brandt and Gao examine the potentially different impacts on crude oil markets from news about macroeconomic fundamentals and geopolitical events. News about geopolitical events shows strong short-run impacts on the crude oil market. In the long run, news about macroeconomic fundamentals acts as a significant predictor of crude oil returns. In contrast, news about geopolitical events only induces uncertainty and higher trading volume (Brandt and Gao 2019).

The sentiment of one news article is highly subjective, assigning sentiment scores to articles manually will inevitably lead to biased sentiment scores. Instead of asking an expert in finance to evaluate the article after reading it, each article's sentiment score should be completely based on a pre-defined scoring rule which is (mostly) independent of each individual article so that the score is as objective as possible. Modern natural language processing (NLP) techniques allow researchers to construct sentiment indices for a large volume of news articles without actually reading all texts. One simplest method of construct objective news sentiment is the dictionary-based method: researchers firstly build a dictionary mapping frequently observed words in financial news articles to their general sentiment. Loughran and McDonald propose a dictionary classifying words into six categories: negative, positive, uncertainty, litigious, modal and constraining (Loughran and McDonald 2011, Bodnaruk, Loughran, and McDonald 2015, Loughran and McDonald 2016). For instance, the word 'bankrupt' is classified as a word carrying negative sentiment in the Loughran-McDonald sentiment dictionary. Then, the algorithm divides the article into single words (the tokenization step) and reduce each word to their lemma (the lemmatization step). For example, the word 'bankruptcy' would be replaced by 'bankrupt'. Afterward, the algorithm counts occurrences of words in the article and calculates the sentiment score based on frequencies of words belonging to each category (e.g., positive and negative words). One potential draw-

back of the dictionary-based method is that it can cover frequently used words only: the Loughran-McDonald covers around 86,000 vocabularies. Another issue is that the dictionary is domain-specific, the dictionary built for the stock market may not be optimal for the crude oil market. Models designed for one market cannot be easily transferred to another market without rebuilding the dictionary. Another method of constructing sentiment is based on word embedding techniques in NLP. The embedding algorithm maps each word to a high-dimensional vector, termed embedding vector, in the embedding space so that words with close meanings would have close embedding vectors. Pennington, Socher, and Manning introduce a Global Vectors for Word Representation (GloVe) algorithm to embed 2.2 millions of commonly used words to 300-dimensional embedding vectors (Pennington, Socher, and Manning 2014). Embedding techniques cover a much wider range of vocabularies compared with dictionary-based methods so that models can be migrated easily.

3 Data

In order to answer research questions, this paper involves two datasets (i) a the daily spot price of crude oil of the West Texas Intermediate (WTI) from which returns are computed, (ii) a news sentiment dataset from Ravenpack News Analytics (RPNA).

3.1 The West Texas Intermediate (WTI) Crude Oil Dataset

West Texas Intermediate (WTI) is a class of light and sweet crude oil that has served as a benchmark for crude oil prices over the past few decades. Cushing, Oklahoma, where the Cushing oil field locates, has been the delivery point for commodities behind crude oil contracts traded at New York Mercantile Exchange (NYMEX). The U.S. Energy Information Administration (EIA) provides daily closing spot prices of WTI crude oil delivered from Cushing. This time series can serve as a benchmark of measuring activities in the global crude oil market.

This paper focuses on crude oil prices between January 1, 2000 and October 31, 2019. Baumeister and Kilian (Baumeister and Kilian 2016) suggest the spot price is highly responsive to news and other macroeconomic shocks, which is exactly the tricky part of forecasting

financial time series. If the proposed forecasting algorithm performs well on the crude oil dataset, such an algorithm is conceivably promising on other datasets as well.

3.2 Crude Oil Returns

This paper focuses on crude oil returns instead of prices for two reasons, (i) accuracy on return prediction can better reflect the potential profitability and (ii) the series of returns is more well-behaved compared with the series of prices.

Specifically, The augmented Dickey-Fuller test on the raw price series gives a p-value of 0.26, which suggests the movement of crude oil prices exhibits significant non-stationarity. Models designed for non-stationarity are much more complex than models for stationary series. Hence the higher computational cost of training these models reduces the profit of any company deploying them. Moreover, the non-stationarity violates assumptions of classical time series models on this dataset, which serve as benchmark models. The efficient market hypothesis cannot be tested without benchmark models.

The closing spot prices of crude oils are available at a daily frequency for weekdays only. Besides weekends, observations are missing on holidays when the exchange market is closed. In following sections, this article refers to these days with valid spot price as **trading days**.

Table 1 reports dates that are most frequently associated with a missing data over the span of 20 years. The set of days with missing data is consistent over these years: the market is always closed on January 1, July 4 (Independence Day) and December 25 (Christmas). Because price data range from January 3, 2000 to October 31, 2019, missing data problems on December 25 are only detected for 19 times in the table. Lastly, the group of dates in late November are responsible for missing data on Thanksgiving holidays since Thanksgiving holiday varies year by year.

Table 1: Top Days with Missing Data

Date	Number of Days with Missing Data
July 4	20
January 1	20
December 25	19
July 3	10
November 23	10
November 24	10
November 25	10
November 22	9
November 26	9

There are only ten weekdays with missing data problem each year on average (3.77% of the entire dataset). The insignificant percentage of missing data allows us to drop those dates without hurting the generalizability of models and experiments in subsequent sections.

For one particular trading day t with closing price p_t, let Δ denotes the gap (in terms of the number of calendar days) between date t and the previous trading day, so that $t - \Delta$ is the last trading day before trading day t. This paper defines the return on day t, denoted as r_t, as the continuously compounded rate of return in equation (3.1).

$$r_t = \frac{\ln(p_t) - \ln(p_{t-\Delta})}{\Delta} \times 100\% \tag{3.1}$$

Moreover, all returns are expressed in percentage points.

The time gap between two observed prices are not uniform. For instance, the return on a Monday can be computed by taking difference between the log close price on Monday and the previous Friday, if available. In this case, $\Delta = 3$. When the previous Friday was not a trading day with valid spot price, $\Delta = 4$ and the return r_t will be $\frac{\ln(p_{\text{Mon}}) - \ln(p_{\text{Prev Thu}})}{4}$.

Table 2: Distribution of Δ by Weekdays

Day of the week	Num. Days.	Num. Trading Days	Δ=1	2	3	4	5
Monday	1,034	931	0	0	887	33	11
Tuesday	1,035	1,023	926	0	0	97	0
Wednesday	1,035	1,027	1,016	5	0	0	6
Thursday	1,035	1,007	999	8	0	0	0
Friday	1,034	990	973	17	0	0	0
Saturday	1,035	0	0	0	0	0	0
Sunday	1,035	0	0	0	0	0	0
Total	7,243	4,978	3,914	30	887	130	17

Table 2 summaries the distribution of Δ values. The Δ values for Mondays are at least 3 because weekend data are always unavailable. One extreme case is that none of Monday and Tuesday is a trading day, so that the Δ value for the Wednesday in this week would be 5. The extreme case occurs rarely for only 6 times during the period of 20 years.

The movement of crude oil returns in the past two decades has exhibited volatile patterns. Figure 1 plots the pattern of returns, in which shaded areas indicate U.S. recessions (March 2001 to November 2001 and December 2007 to June 2009). Noticeably, crude oil returns are more volatile during recession periods and are becoming even more volatile in recent years.

Figure 1: Crude Oil Returns

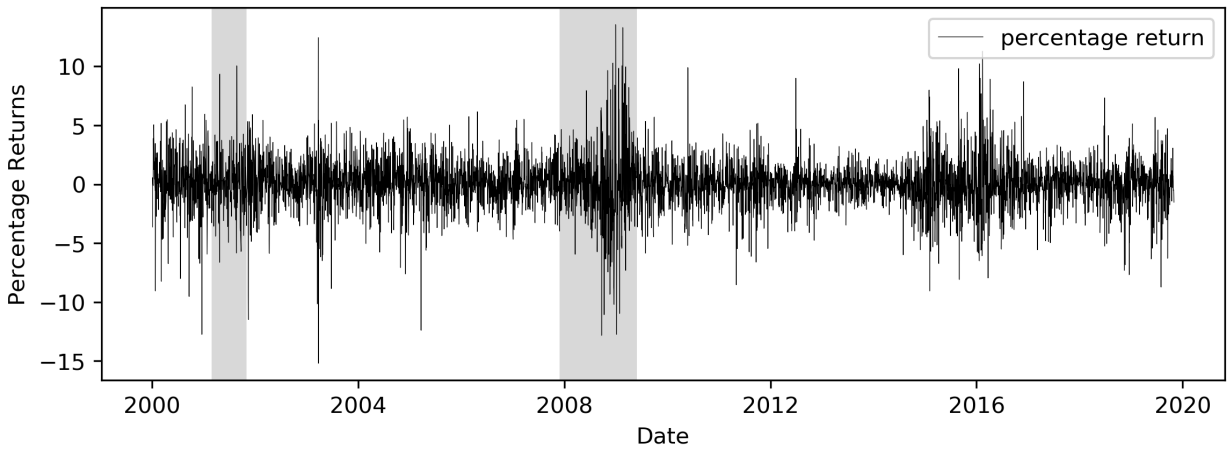

Table 3 reports summary statistics for the percentage crude oil returns, in which normal-

ized skewness and excess kurtosis are defined as

$$\hat{m_3} := \frac{\frac{1}{n}\sum_{i=1}^{n}(x_i - \bar{x})^3}{\sigma_x^3} \text{ (normalized skewness)} \tag{3.2}$$

$$\hat{m_4} := \frac{\frac{1}{n}\sum_{i=1}^{n}(x_i - \bar{x})^4}{\sigma_x^4} - 3 \text{ (excess kurtosis)} \tag{3.3}$$

$$\text{where } \sigma_x := \sqrt{\frac{1}{n}\sum_{i=1}^{n}(x_i - \overline{x})^2} \tag{3.4}$$

Summary statistics in the Table 3 suggest the mean return within each year are nearly zero, which agrees the conventional expectation that returns are zero on average. During periods of recessions, the average returns are below -0.2%,. Moreover, during same period, the series becomes significantly more volatile as well. Given the high kurtosis between 2008 and 2009, one are more likely to encounter extreme returns, both positive and negative, during recession periods.

Table 3: Summary Statistics for Crude Oil Returns

Year	Obs.	Mean	Median	Std.	Min	Max	Normalized Skewness	Excess Kurtosis
2000	249	0.03433	0.20148	2.61996	-12.74152	8.26343	-0.92174	3.45580
2001	250	-0.02409	-0.04434	2.54058	-11.48581	10.05107	-0.06444	3.15304
2002	250	0.15535	0.15221	1.70283	-5.86460	5.43272	-0.22297	0.62431
2003	250	0.07861	0.13203	2.57315	-15.19090	12.44253	-0.89439	7.30189
2004	249	0.08918	0.11605	2.08792	-7.60501	5.70121	-0.38117	1.01395
2005	251	0.05257	0.11019	1.96717	-12.39009	5.02715	-1.04498	5.84007
2006	249	-0.00539	0.12995	1.58949	-4.45214	6.15402	0.13487	1.03258
2007	252	0.23400	0.09798	1.69800	-4.66915	5.51381	0.13705	0.65946
2008	253	-0.29945	-0.07920	3.34992	-12.82672	13.54551	-0.01650	2.60308
2009	252	0.26537	0.19157	2.92040	-12.74310	13.29544	0.29333	4.25972
2010	252	-0.02077	0.03198	1.74554	-5.18874	9.89802	0.39313	3.82001
2011	252	0.00583	0.10994	1.94170	-8.53498	5.18170	-0.69170	2.27400
2012	252	-0.04164	0.03600	1.51078	-4.76060	9.00091	0.54820	5.53225
2013	252	0.01455	0.04489	1.06690	-3.46951	3.20999	0.05495	0.67398
2014	252	-0.16510	-0.05343	1.36052	-5.98638	4.91592	-0.76983	3.16348
2015	252	-0.03610	-0.25616	2.63361	-9.05140	9.81397	0.24129	1.25225
2016	252	0.20931	0.00000	2.79698	-7.95603	11.28922	0.70466	2.11826
2017	250	0.06564	0.17286	1.40987	-5.56187	3.32016	-0.87368	2.07271
2018	249	-0.10076	0.07393	1.81925	-7.67683	7.33414	-0.64252	3.38603
2019	210	0.04359	0.10073	1.93931	-8.72444	5.67862	-0.66251	2.87153
2000∼2019	4978	0.02754	0.06307	2.15250	-15.19090	13.54551	-0.16152	5.12757

Figure 2: ACF and PACF for Crude Oil Returns (missing data dropped)

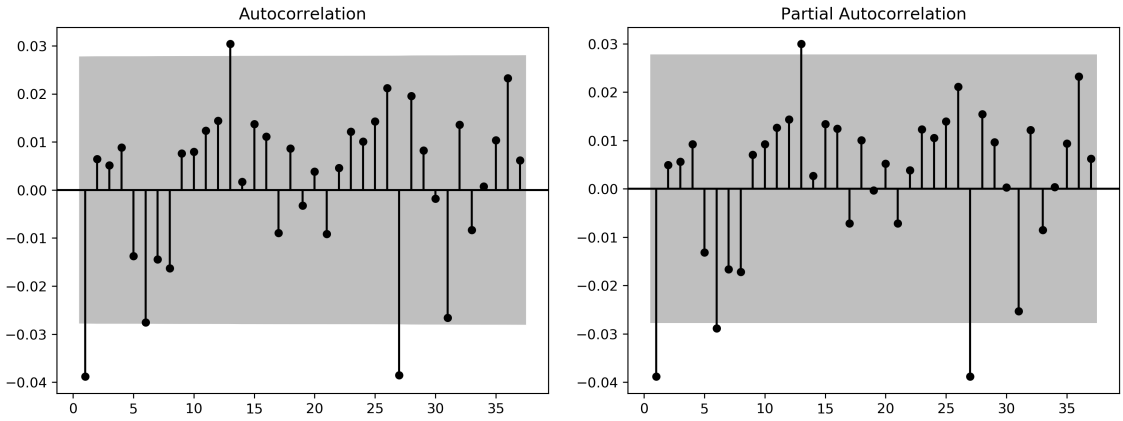

The autocorrelation function (ACF) and partial autocorrelation function (PACF) plots in Figure 2 explore the inter-temporal correlation within the return series. Since only a few lags are statistically significant in the ACF and PACF plots, we do not expect linear time series models are capable to achieve high performances in this return prediction task.

It is worth noticing that lag 1, 6, 13, 27 are significant in both ACF and PACF plots, which may indicate seasonalities with period of one week. However, regularity in missing data can lead to this observation as well. Hence, instead of dropping days with missing data, we fill up these missing data using random values from a Gaussian distribution parameterized by the mean and variance of the entire dataset. Figure 3 plots the ACF and PACF of return series with missing values filled using random noise, the significance at lag 6 disappeared, but the significance of bi-weekly lag persists and another spike at lag 36 emerges. This observation indicates that there might be seasonality with bi-weekly periods. In the experiment section, we are going to examine seasonal models with both period lengths.

Figure 3: ACF and PACF for Crude Oil Returns (missing data filled)

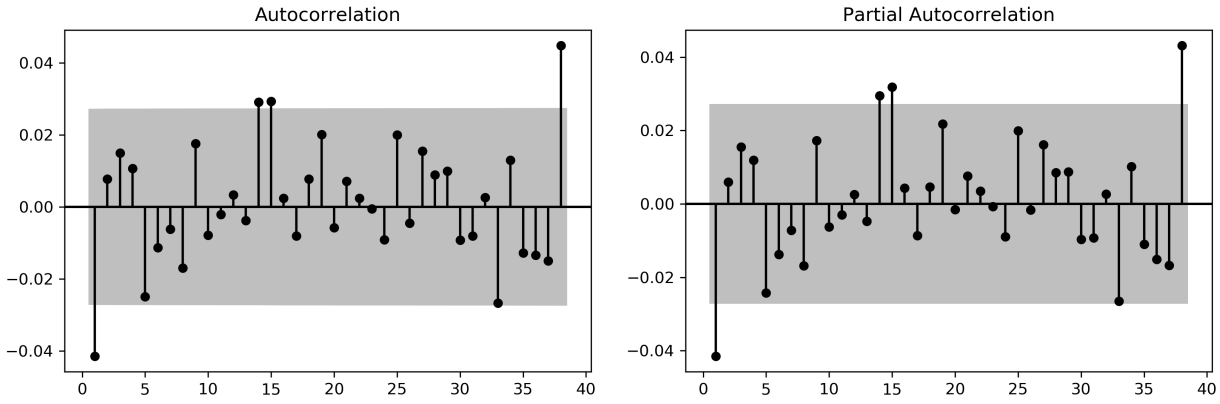

The histogram in Figure 4 suggests that the empirical distribution of crude oil returns is much clustered near zero than a Gaussian distribution. With this clustering feature, conventional metric for evaluating regression models, such as mean squared error (MSE), will not be sufficient in this task. For instance, a dummy model consistently predicting zero will attain a fair MSE (to be specific, the variance of entire dataset). Therefore, in later sections, we introduce another directional accuracy to assess the fitness of models.

Figure 4: Distribution of Crude Oil Returns

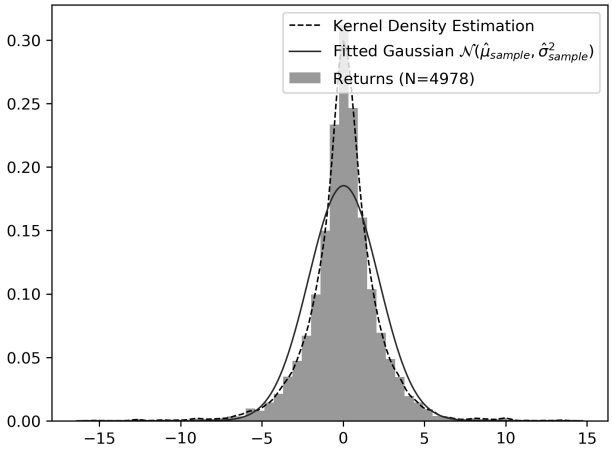

3.3 Day of the Week Effect in Crude Oil Dataset

3.3.1 Difference in Returns across the Week

Gibbons and Hess (1981) examined returns on stocks from S&P 500, Dow Jones 30, and Treasury Bills. They found strong negative mean returns on Monday compared with other weekdays. The seasonality persisted even after taking market adjustment measures, such as using mean-adjusted returns instead (Gibbons and Hess 1981). Analysis in this paper unveils a similar daily seasonality presents in crude oil returns as well. Panels in Figure 5 demonstrate the empirical distributions of returns on each day of the week and Ns within parentheses in captions denote the number of observations. We can see that Mondays and Wednesdays have relatively larger variances, which again matches Gibbons and Hess' observations.

Figure 5: Distributions of Returns on Each Day of the Week

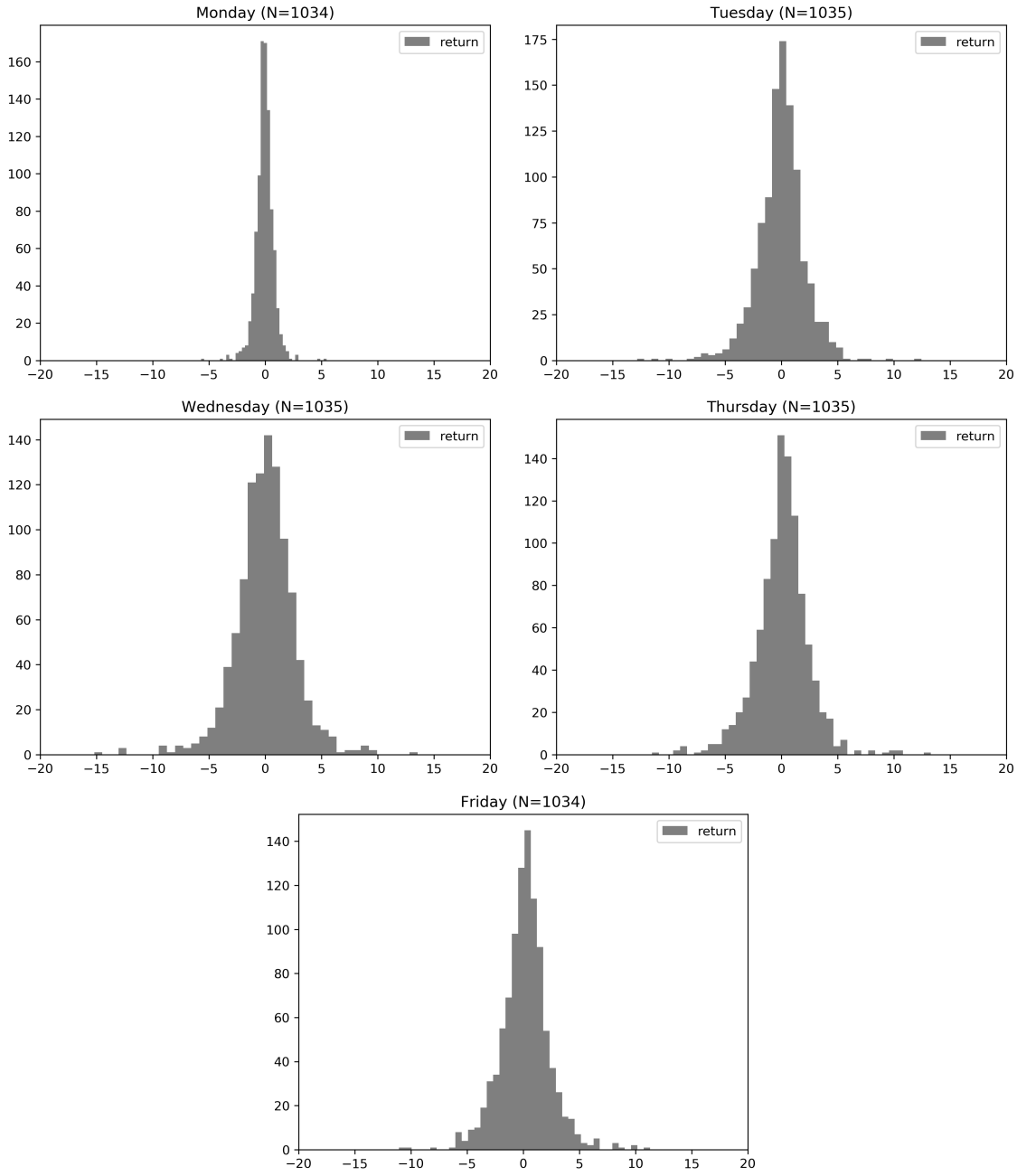

Table 4 below provide summary statistics for prices and returns on each day. [1] It turns out that at a significance level of 0.05, Monday and Friday are the only two weekdays with a mean return significantly different from than zero. And the t-test suggests Mondays are

[1] In Table 4, a value of -0.000 indicates a negative value with magnitude less than 0.0005. P-values are calculated in a two-tailed t-test with null hypothesis $\mu_0 = 0$. Bold fonts indicate statistically significance at level $\alpha = 0.05$.

more likely to associate with negative returns, meanwhile, Friday is more often associated with positive returns.

Table 4: Summary Statistics of Crude Oil Returns on Each Day of Week

Day of the week	Num. Obs.	Mean (P-Value)	Std.	Normalized Skewness	Excess Kurtosis
Monday	931	**-0.055 (0.042)**	0.816	-0.134	7.088
Tuesday	1,023	-0.034 (0.615)	2.141	-0.335	4.214
Wednesday	1,027	-0.000 (0.998)	2.660	-0.325	3.798
Thursday	1,007	0.069 (0.361)	2.378	-0.041	3.64
Friday	990	**0.155 (0.026)**	2.194	0.128	3.243
Total	4,978				

3.3.2 Kolmogorov-Smirnov test for Distributional Similarities

Smirnov developed a non-parametric method of testing the equality between two continuous distributions, with CDFs $F(x)$ and $G(x)$ respectively (1939). Hodges' work provided more details on the Kolmogorov-Smirnov test and relevant methods (1958). I am using the two-tailed version of Kolmogorov-Smirnov test to check whether distributions of two different days are similar. Given two datasets, take returns on Mondays and Tuesdays for example, the null hypothesis says those two datasets are drawn from the same distribution, and the alternative says they are from different distributions. [2] Firstly, the Kolmogorov–Smirnov test constructs the empirical CDFs $F_{Mon,927}(x)$ and $F_{Tue,1018}(x)$ from the dataset. Then, the Kolmogorov–Smirnov statistic measures the maximum discrepancy between two distribution functions, which is

$$D := \sup_x |F_{Mon,927}(x) - F_{Tue,1018}(x)| \in [0,1] \tag{3.5}$$

A smaller D-statistic implies stronger distributional similarity between two distributions. For instance, when $F_{Mon,927}(x)$ and $F_{Tue,1018}(x)$ are exactly the same, the D-statistic is zero. In contrast, let $X = 0$ and $Y = 1$ be two "deterministic" random variables, in this case,

[2] Different alternative hypotheses can be used in Kolmogorov–Smirnov test: i) $H_1 : F(x) \geq G(x)$, ii) $H_1 : F(x) \leq G(x)$, and iii) $H_1 : F(x) \neq G(x)$. This paper is using the third (two-tailed) alternative hypothesis.

there distributions are completely different, and $D_{X,Y} = 1$.

The test rejects H_0 at a significance level of α if

$$D > \sqrt{-\frac{1}{2}\ln\frac{\alpha}{2}}\sqrt{\frac{n+m}{nm}} \tag{3.6}$$

where m and n denote sizes of two datasets.

Table 5: D-Statistics in Kolmogorov-Smirnov Tests

D-Statistic (P-Value)	Monday	Tuesday	Wednesday	Thursday	Friday
Monday	0.000(1.000)	**0.193(0.000)**	**0.243(0.000)**	**0.189(0.000)**	**0.180(0.000)**
Tuesday		0.000(1.000)	0.064(0.030)	0.064(0.030)	**0.071(0.010)**
Wednesday			0.000(1.000)	0.058(0.062)	**0.084(0.001)**
Thursday				0.000(1.000)	0.030(0.729)
Friday					0.000(1.000)

Table 6: The Kolmogorov-Smirnov D-Statistic for all pairs of distributions. Bold font indicates the null hypothesis is rejected at a significance level of 0.01, which implies discrepancy in distributions.

Table 5 presents the Kolmogorov-Smirnov D-Statistic for distributions of every pairs of days. At a significance level of 0.05, we can see that Mondays follow a distribution significantly different from distributions of other weekdays follow. Because the dataset does not contain weekend data, returns on Mondays is always computed using the difference between log prices on Monday and the previous Friday (Thursday if Friday is not a trading day and so on). Therefore, returns associated with Mondays pick the weekend effect. In fact, the distribution of returns on Mondays (over weekends) is the only one with negative mean among distributions of all five days.

3.4 News Sentiment Dataset

The event sentiment dataset from RavenPack News Analytics (RPNA) tracks and analyzes all information of companies, organizations, countries, commodities, and currencies from four major sources: Dow Jones Newswires, Wall Street Journal, Barron's and MarketWatch. This dataset covers events from January 1, 2000, to October 30, 2019. RavenPack records the exact date and coordinated universal time (UTC) when each news article is published. Since

the crude oil prices are from New York Exchange (NYEX), which uses US Eastern time, this UTC time is converted into Eastern time.

This paper defines one **news item** to be one news article included in the RPNA dataset. One news item is a concrete published article associated with a headline, body text, a date when it is published and other information. In the following discussion, I am using news items, pieces of news, news articles or simply news interchangeably but all of them are equivalent to news items.

Each piece of news in the dataset is assigned with a topic based on its headline and text. In order to filter out noisy and irrelevant information, this paper works on the subset of news with crude oil topic as the main source of news. It turns out that there are 106,960 news article from the original dataset have a topic of crude oil, this results in 17 piece of news per day on average.

Noticeably, there could be multiple news articles reporting the same event and this could lead to duplicate counting problems. Later in this section, an alternative measure of news sentiment is constructed to mediate this problem.

Table 7 provides summary statistics of numbers of news about crude oil reported each day by years. In 2004, 2008 and 2012, crude oil topic is relatively hot and there were about 20 news about crude oil in these years. In contrast, publishers are quieter in 2002, 2003 and recent years.

Table 7: Summary Statistics for Daily Numbers of News Items Arrived by Years

Year	Mean	Median	Std.	Min	Max	Normalized Skewness	Excess Kurtosis
2000	8.665	8.000	8.315	0.000	48.000	1.228	1.939
2001	11.493	11.000	10.247	0.000	51.000	0.682	0.059
2002	3.542	3.000	3.642	0.000	19.000	1.403	2.368
2003	5.126	3.000	6.145	0.000	39.000	2.058	5.646
2004	20.776	19.000	17.680	0.000	84.000	0.728	0.193
2005	17.473	17.500	13.796	0.000	57.000	0.403	-0.460
2006	18.615	19.000	14.272	0.000	58.000	0.247	-0.862
2007	16.781	16.000	13.669	0.000	66.000	0.567	-0.187
2008	20.500	22.000	15.141	0.000	66.000	0.304	-0.562
2009	14.499	14.000	10.988	0.000	48.000	0.296	-0.761
2010	15.564	17.000	11.437	0.000	52.000	0.247	-0.753
2011	19.187	20.000	14.175	0.000	65.000	0.231	-0.610
2012	20.077	22.000	14.682	0.000	65.000	0.206	-0.688
2013	14.526	15.000	11.364	0.000	57.000	0.413	-0.374
2014	13.353	11.000	13.445	0.000	69.000	1.502	2.596
2015	18.663	18.000	15.974	0.000	80.000	0.738	0.188
2016	19.956	18.000	17.454	0.000	101.000	0.837	0.661
2017	12.479	11.000	10.927	0.000	58.000	0.797	0.619
2018	13.277	13.000	11.490	0.000	93.000	1.350	5.481
2019	10.505	9.000	10.608	0.000	65.000	1.067	1.569

In general, weekends are quiet period of news arrival, while much more news arrive in the middle of each week. Figure 6 summarizes the average numbers of news on each day of the week, and Table 8 summarizes the average number of news on each day in each year. It turns out that weekends are much quieter than weekdays and only less than 5 % of all news are reported on weekends. Moreover, the number of news arrivals peaks on Wednesday in all years but 2000 and 2002.

Figure 6: Average Numbers of News on Each Day of Week

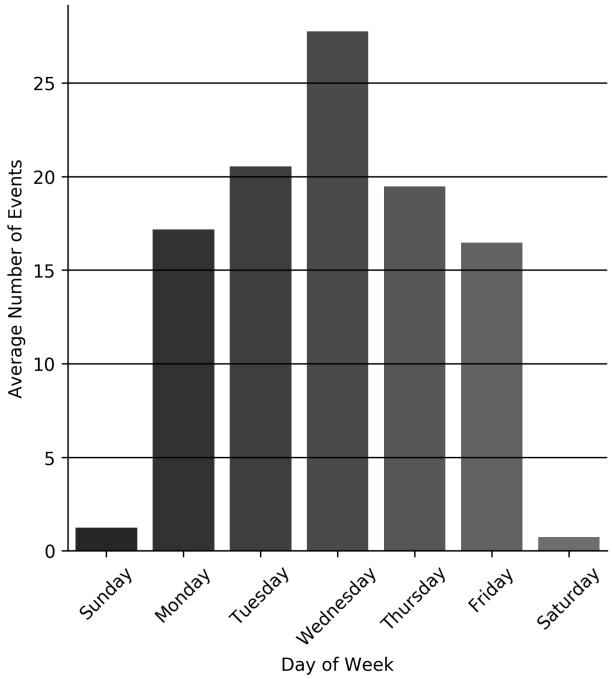

Table 8: Average Numbers of News Items Published on Each Day of Week in Each Year

Year	Monday	Tuesday	Wednesday	Thursday	Friday	Saturday	Sunday
2000	11.157	14.135	13.077	11.885	9.769	1.643	1.500
2001	12.547	17.569	21.327	15.058	14.078	1.000	1.200
2002	5.771	5.019	5.224	3.980	5.469	1.200	1.600
2003	7.080	6.529	9.942	6.863	5.490	1.200	1.136
2004	24.058	28.981	39.250	28.660	22.302	2.182	2.240
2005	21.462	21.846	33.596	24.654	19.000	1.765	2.259
2006	22.981	24.885	35.904	24.846	19.731	1.346	2.161
2007	19.792	21.385	33.577	23.846	16.769	1.941	2.212
2008	24.788	26.415	36.415	26.269	25.250	2.207	3.065
2009	16.058	21.346	29.192	16.925	15.538	1.688	2.366
2010	16.327	23.058	28.654	20.596	17.135	2.261	2.932
2011	23.769	28.577	32.904	25.750	19.942	2.053	3.441
2012	22.340	26.654	36.423	26.981	25.118	3.783	2.756
2013	16.673	19.642	28.588	19.038	15.846	2.500	2.366
2014	15.510	18.846	25.113	16.923	15.529	2.167	2.467
2015	23.019	27.135	35.558	23.189	19.843	2.091	2.957
2016	23.333	29.192	38.462	24.808	23.077	2.190	2.105
2017	14.220	16.788	25.192	16.077	14.039	1.696	1.667
2018	13.654	19.059	24.712	18.635	15.235	2.586	2.143
2019	11.263	15.872	24.600	15.026	13.795	1.923	1.500

3.4.1 Event Sentiment Scores

To estimate the potential economic impact upon news arrival and afterwards, Ravenpack assigns each piece of news an **Event Sentiment Score** (ESS) between 0 and 100 using a proprietary algorithm combines results from surveying financial experts and pattern matching. An ESS of 100 indicates extreme positive short-term positive financial or economic impact. In contrast, an ESS with zero value indicates extreme negative impact. And a ESS of 50 indicates exact neutral news, which indicates noise.

Raw scores (range from 0 to 100) are calibrated by subtracting 50, so that positive (negative) news items always have positive (negative) score and a zero score represents a neutral news.

The first panel in Figure 7 plots the distribution of (normalized) ESS for all news about crude oil, while second and third panels focus on two tails of the distribution. From the histogram in Figure 8, one can see that only a small portion of news is purely neutral with zero ESS (3,479 news items, 3.25 % of all news). Moreover, ESS scores of most news are clustered around -15 (39,347 news items, and 36.8 % of all news) and 18 (34,574 news items and 32.3 % of all news). Analyzing contents of these news suggests they are simply objective reports of past price/return movements of crude oil commodities and futures. Therefore, I do not expect these news to provide as much information on predicting returns as other breaking news like OPEC export restrictions. In order to emphasize fresh events other than reports of past price movements, models proposed in this paper will focus on extreme events by assigning them higher weights. Specifically, models are designed to pay more attention to news carrying sentiment scores with high absolute values, meanwhile, models actively discriminate news whose sentiment scores are near zero.

Figure 7: Distribution of Event Sentiment Scores (ENS)

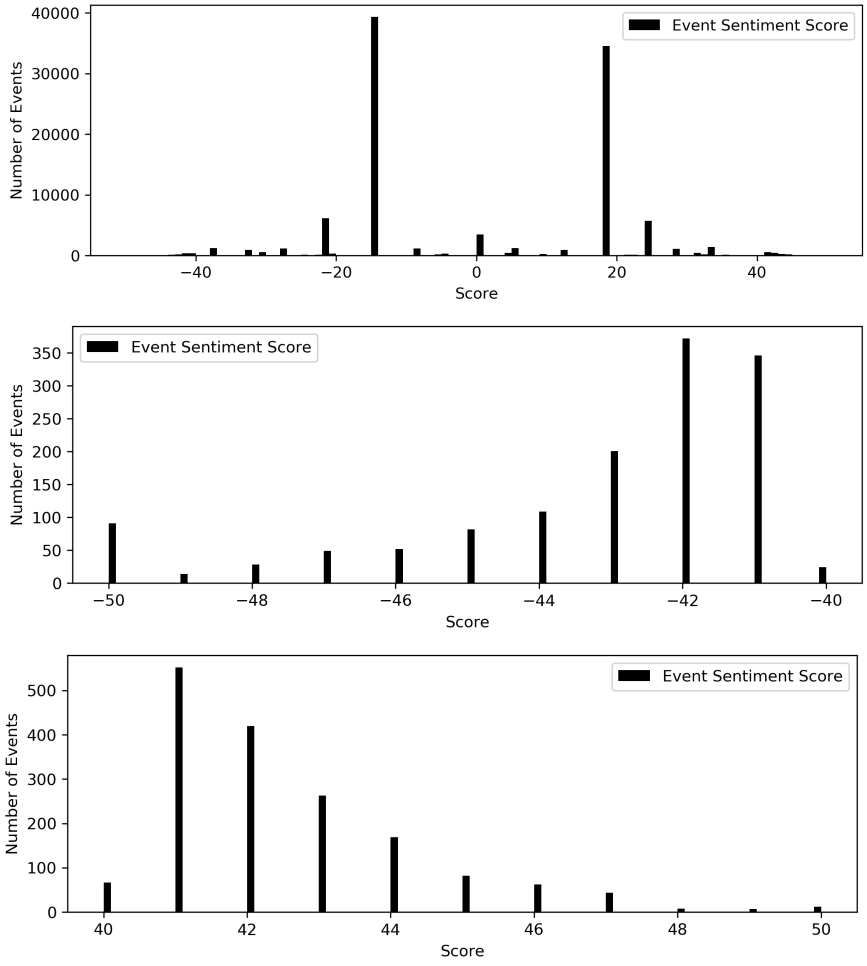

Figure 8 plots the distribution of ESS scores in each year. The pattern of clustering around -15 and 18 is pretty consistent over the span of 20 years: the majority of news are simply reporting the crude oil market instead of events outside the market.

Figure 8: Distribution of Event Sentiment Scores (ENS) each Year

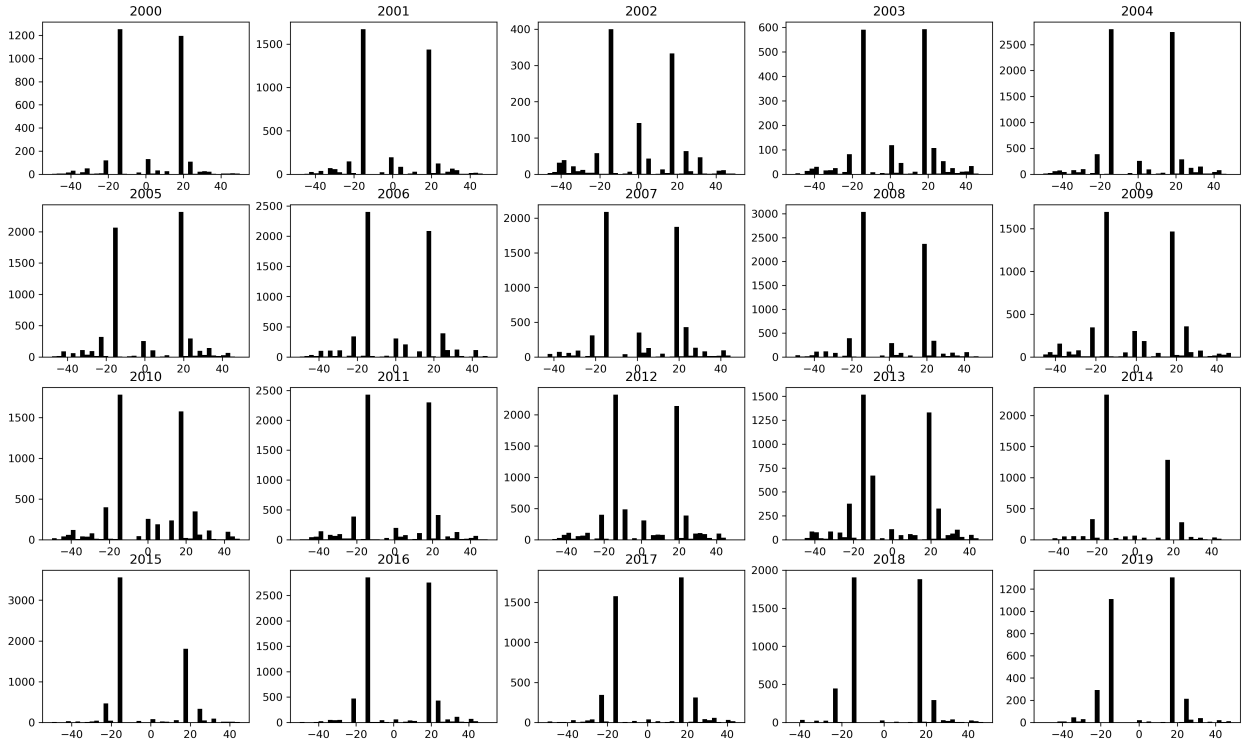

3.4.2 Weighted Event Sentiment Scores

Different news sources report the same event so that there are duplicate entries about the same event in this dataset, which aggravates the problem of noise. RPNA dataset computes an **Event Novelty Score** (ENS) to measure how novel a news story is within a 24-hour period.

Suppose that OPEC announces an export resection after a conference finished at 11:00 a.m. January 10. After 30 minutes (11:30 a.m., January 10) one news source reports this export cut, and this news article is one entry in the dataset. To determine the ENS of this news article, the algorithm looks into the 24-hour period prior to the news arrival, that is, from 10.30 a.m. January 9 to 10.30 a.m. January 10. If there is no news about this export restriction in this period, then this news article is the first report of this export cut event and receives an ENS score of 100. In contrast, if there are another two articles about the same events published before this articles, this article is the third one and receives a decayed novelty score of $100 \times 0.75 \times 0.75 = 56$ instead.

In general, the ENS decays exponentially as there are more news reporting the event. For an arbitrary news article i, if there are another k articles of the same topic published within the 24-hour period before article i arrives, article i is therefore the $k + 1^{th}$ articles on this topic and would receive a novelty score of

$$\text{ENS}_i = 100 \times 0.75^k \tag{3.7}$$

Figure 9 plots the distribution of ENS, the histogram suggests that most news have relatively high novelty scores.

Figure 9: Distribution of Event Novelty Score

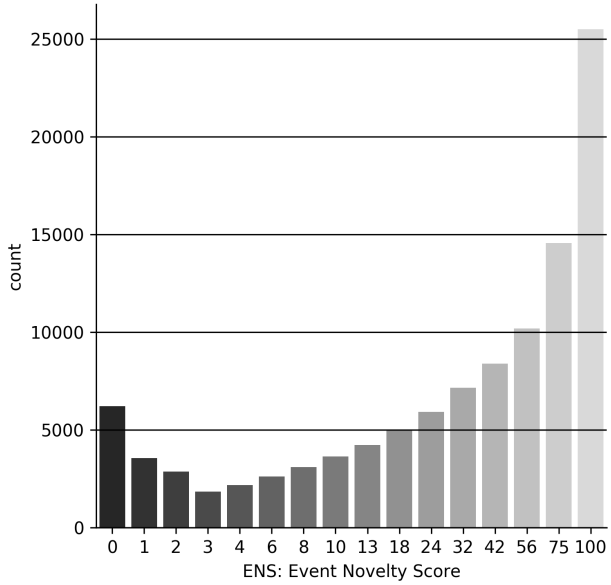

To address the duplication issue, this paper constructs an alternative metric of sentiment, **Weighted Event Sentiment Score** (WESS), from both ESS and ENS.

$$\text{WESS} := \frac{\text{ESS} \times \text{ENS}}{100} \tag{3.8}$$

We divide the product of ESS and ENS in equation (3.8) by 100 so that WESS ranges from -50 to 50 as well.

The constructed WESS scores have several advantages for modelling. Firstly, WESS discriminates against duplicate news articles. For example, if one extreme negative event

with an ESS of - 50 happened, many sources report this event within 24 hours after it happened. The sum of ESS of all these news would overestimate how bad the scenario is because the negative event only occurs once but it is reported for several times. Weighting ESS of articles using their novelty scores helps mitigate this problem so that WESS allows models to pay more attention on novel news rather than redundant ones. Secondly, WESS preserves the sign of ESS, so that an event carries positive sentiment, in terms of ESS, if and only if its WESS score is positive.

The histograms in Figure 10 illustrate the overall distributions of WESS as well as the two tails of it. It turns out that the clustering pattern in Figure 7 disappears and much more news are now with zero sentiment scores. Therefore, WESS provides a stricter filter to filtering out noises (i.e., news with zero sentiment scores) and better helps models to focus on meaningful news only.

Figure 10: Distribution of Weighted Event Sentiment Scores (WESS)

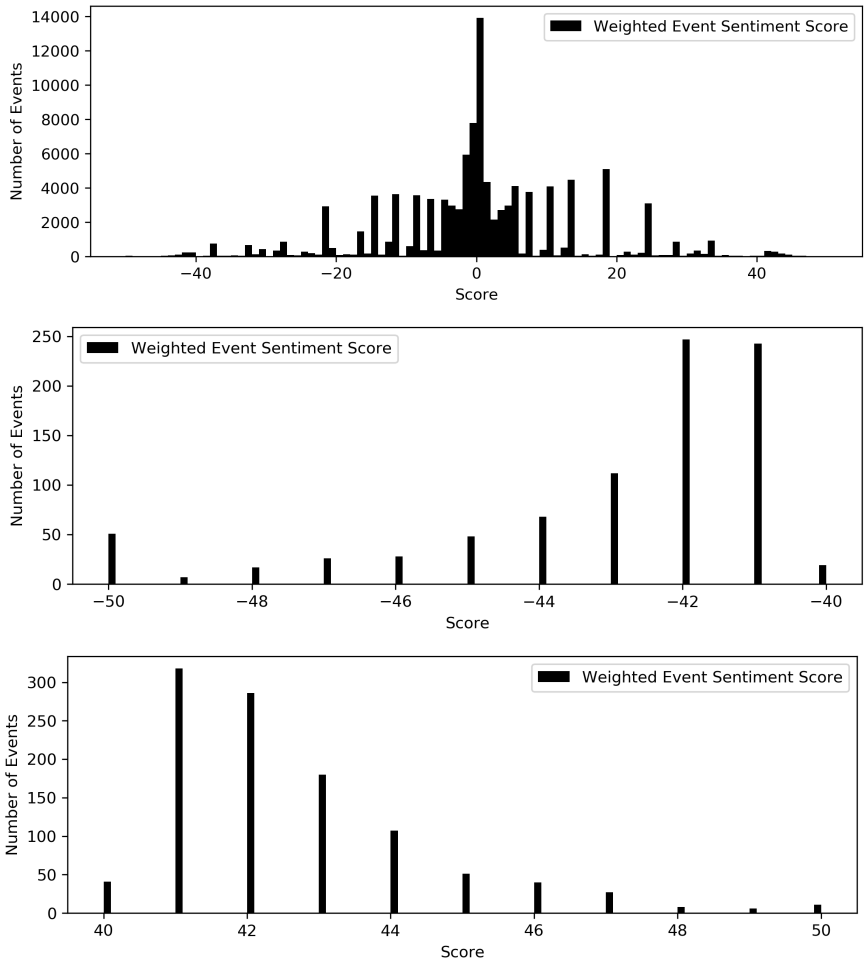

Figure 11 plots the yearly distributions of WESS. The yearly distributions suggest that there are more events with negative sentiments in 2001 as well as in 2008-2009, such observation matches the US recession records in Figure 1.

Figure 11: Distribution of Weighted Event Sentiment Scores (WESS) each Year

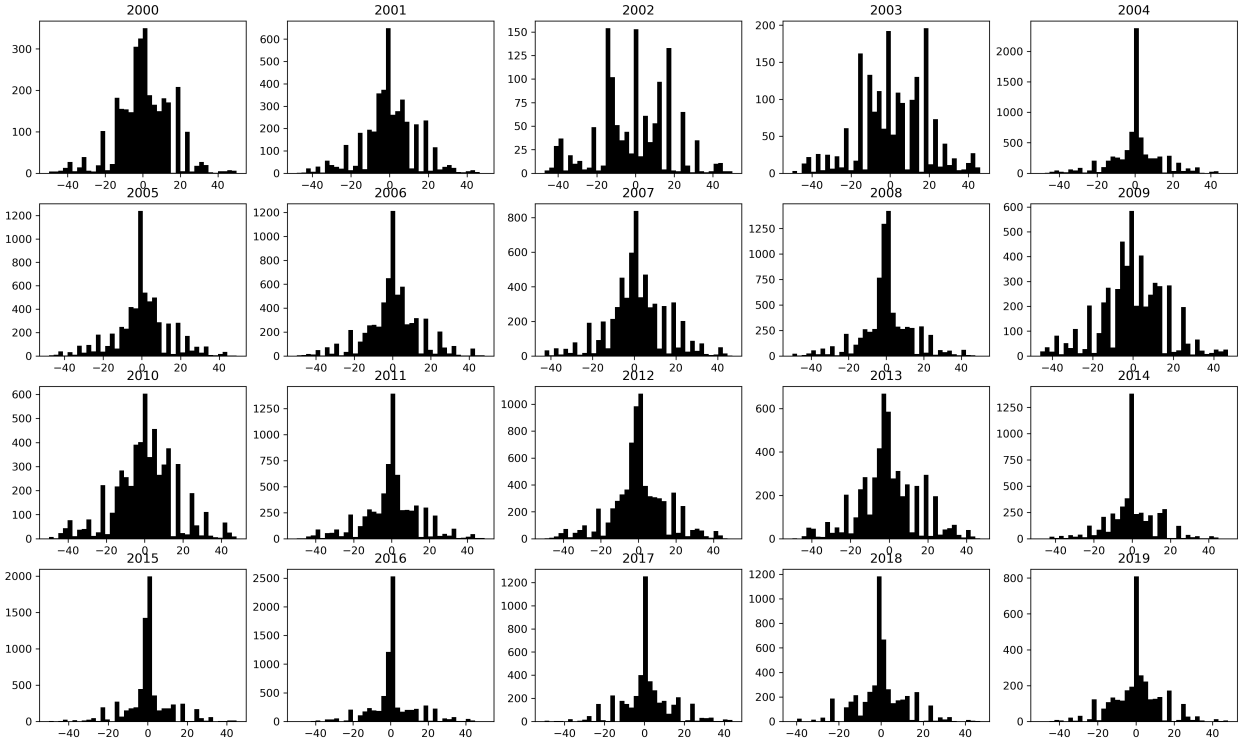

3.4.3 Time of News Arrival

The numbers of news arrived are not evenly distributed across the timeline, there are always busy hours as well as quiet hours. Figure 12 summarizes the average number of news arrives on each day over the period of 20 years. The trench at the end of February corresponds to leap years. Other trenches are in general correspond to holidays, for example, average numbers of news on the Independence Day and Christmas are significantly less than other days.

Figure 12: Average Number of Events on Each Day

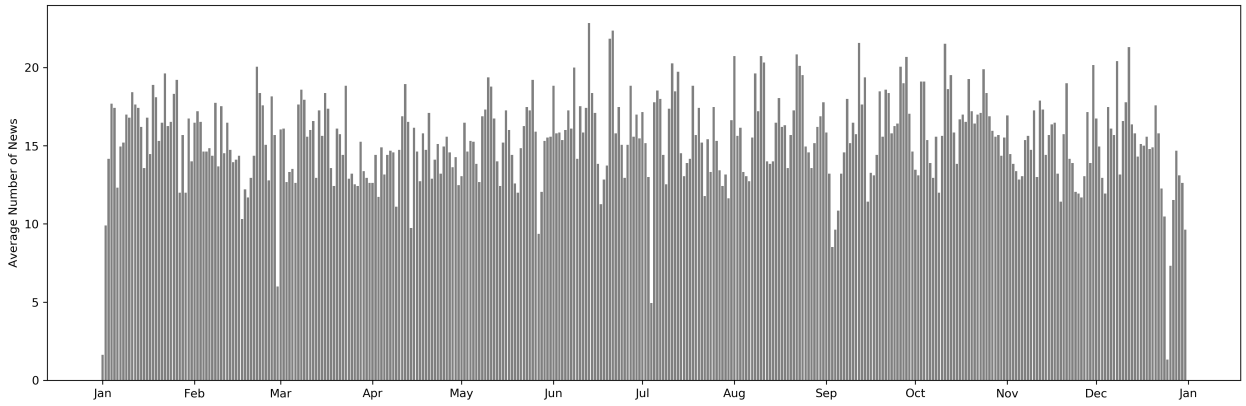

Figure 13 has a look at the distribution of news arrival within 24 hours. It is worth noticing that, in the RPNA dataset, the original timestamps recording when news arrives are using Universal Time Coordinated (UTC). To incorporate the crude oil dataset, we convert raw timestamps to Eastern Standard Time (EST) timezone[3], where crude oil commodities are traded. From the distribution of news arrival, one can see that most news arrive during day time between 10:00 and 16:00. There is an unusual spike at 2:00, this could correspond to morning news at 7:00 in British. But because all four news sources in RPNA dataset are U.S. based publishers, the news arrival process is quiet again between 3:00 and 9:00 as less reporters are actively writing during this time.

Figure 13: Total Number of News Arrived

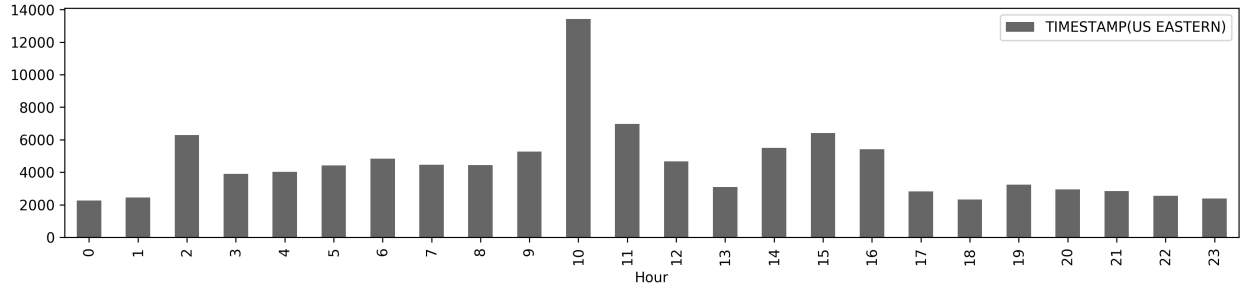

In order to have a closer look at the intertemporal correlation of event sentiment, this

[3]EST is five hours behind UTC during autumn and winter. During spring and summer (daylight saving time), EST is four hours behind UTC.

paper firstly compute the mean event sentiment score of all events within each day, denoted as $\overline{\text{ESS}}$ and $\overline{\text{WESS}}$ respectively, in the span of 20 years. The ACF and PACF plots of the daily average ESS in Figure 14 suggest the intertemporal correlation here is much more salient than the series of returns, which has only a few significant lags.

Figure 14: ACF and PACF of $\overline{\text{ESS}}$

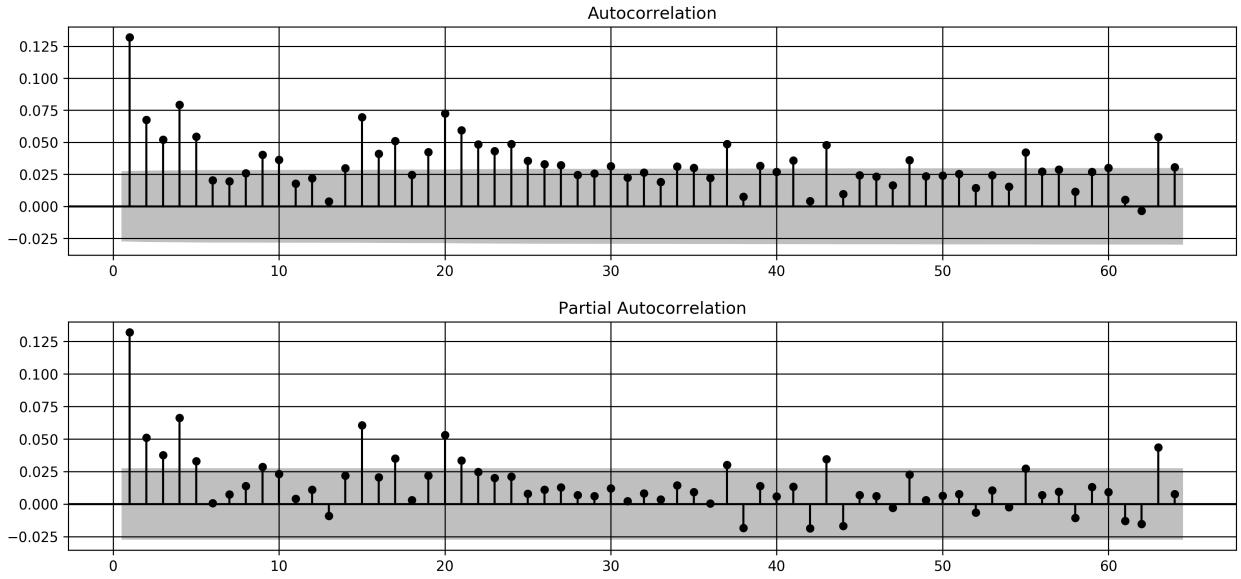

Moreover, there exists significant correlation between the price movement series and news sentiment. Figure 15 plots the trends of daily average sentiment and crude oil returns in 2019, in which these two series have shown significant co-movement pattern. It turns out that the Spearman correlation between these two series is 0.562 with p-value zero.

Figure 15: Movements of $\overline{\text{ESS}}$ and Return in 2019

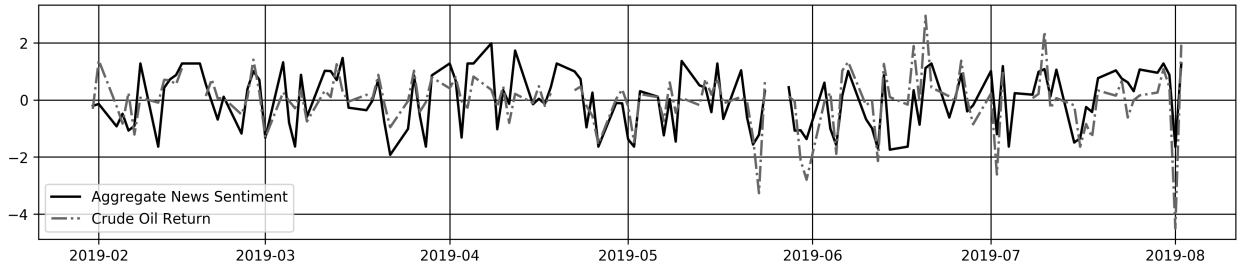

This co-movement provides justification of using the series news sentiment to predict crude

oil returns.

3.5 Classifying News Type

Based on the distributions shown in previous sections, we shall see that a great number of events carry nearly natural sentiment or are just description of past price movement. This paper wishes to allow models to differentiate different types of news instead of taking the average sentiment score of all news. As seen in the histograms of sentiment scores (figure 7 and 10), the distributions are pretty much symmetric about zero, therefore, for simplicity, this paper assumes the region of neutral news to be symmetric around zero. Specifically, the classification procedure firstly determines a radius $r \geq 0$. Afterward, the algorithm classifies all news based on their (weighted) event sentiment scores. News with score (W)ESS $\in [-50, -r)$ are negative news, and all news with (W)ESS $\in (r, 50]$ are positive news, and, news in $[-r, r]$ are neutral news. Figure 16 and Figure 17 plots the composition of news types while classifying these news using two criterions, event sentiment scores and weighted event sentiment scores.

Figure 16: Composition of News Type based on ESS

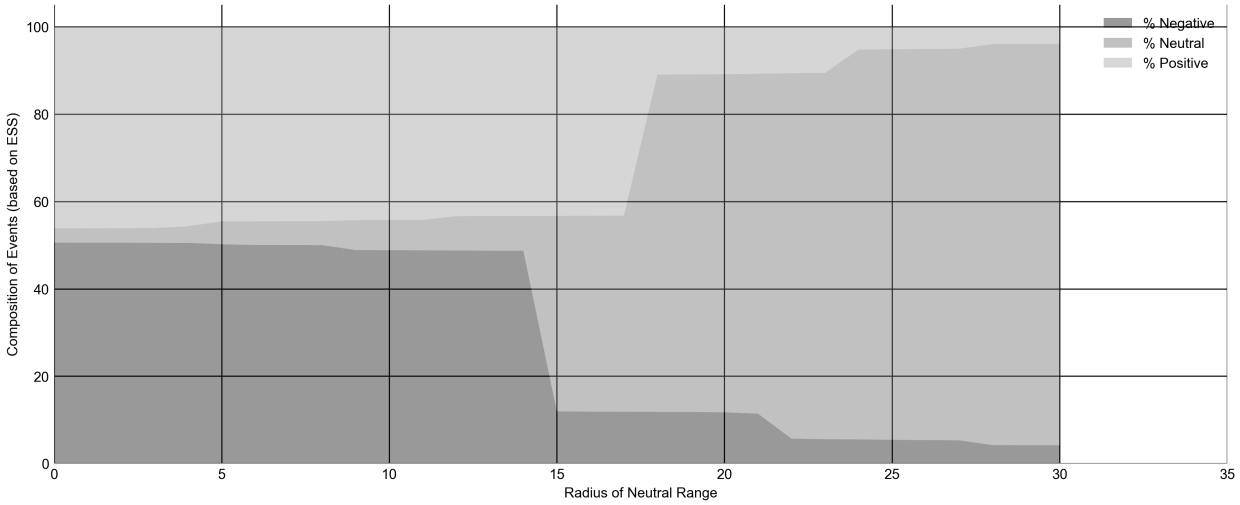

Figure 17: Composition of News Type based on WESS

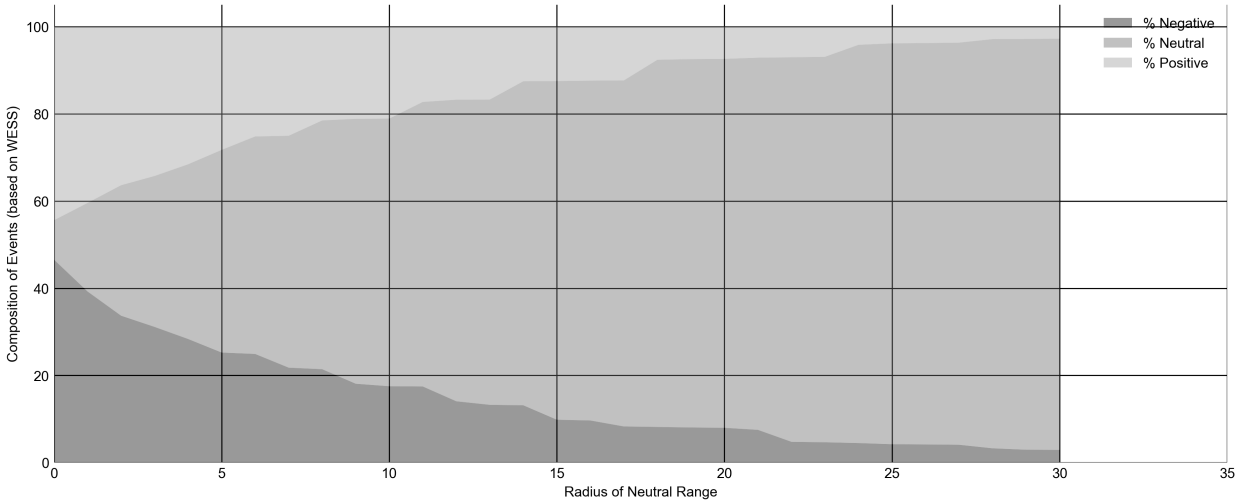

In Figure 16, the two sharp breaking points at $r = 15$ and $r = 18$ correspond to the two clusters of events with sentiment scores 35 and 68 observed in Figure 7. Table 9 and Table 10 summarizes how the portions of different classes of news change while applying different value of threshold.

For example, if one decides to classify news based on their WESS scores and a radius $r = 0$. Then news with strictly positive (negative) WESS would be classified as positive (negative) and one piece of news is neutral only if it has exactly zero WESS. In this case, 46.54 % (44.4 %) of all news are classified as positive (negative) and the rest 9.06 % of news are neutral (the first row in Table 10). This paper refers this composition of news resulted from using $r = 0$ as the reference composition. Similarly, the classification criterion using WESS and $r = 10$ will firstly construct a closed interval $[-10, 10]$. Then any news with ESS scores fall in $[-10, 10]$ would be classified as neutral news and news will ESS scores less than -10 and greater than 10 are classified as negative and positive respectively. In this case, 17.51 % of news are classified as negative news, this percentage shrinks to $\frac{17.51\%}{46.54\%} = 37.64\%$ compared with the reference composition. In contrast, 61.39 % of news are now labelled as neutral news and this percentage is $\frac{61.39\%}{9.06\%} = 677.67\%$ of the neural percentage in the reference composition (the sixth row in Table 10).

In the appendix, Table 32 and 33 provide a more complete summary on the composition

of news under various thresholds r. The threshold variable r is a hyper-parameter in our model, the optimal classification threshold depends on specific type of models used. In most experiments, we are using $r = 0$ for ESS scores and $r = 0.3$ for WESS scores.

Table 9: Composition of News Classes with Different Thresholds on ESS Scores

r	Num Negative	Num Neutral	Num Positive
0	50.59% (100.00%)	3.25% (100.00%)	46.15% (100.00%)
0.3	50.59% (100.00%)	3.25% (100.00%)	46.15% (100.00%)
1	50.57% (99.96%)	3.29% (101.24%)	46.13% (99.96%)
3	50.52% (99.85%)	3.39% (104.08%)	46.09% (99.87%)
5	50.20% (99.23%)	5.24% (161.14%)	44.55% (96.54%)
10	48.84% (96.53%)	6.91% (212.45%)	44.25% (95.88%)
15	11.93% (23.58%)	44.76% (1376.20%)	43.31% (93.83%)
20	11.73% (23.18%)	77.41% (2379.79%)	10.87% (23.55%)
25	5.41% (10.70%)	89.43% (2749.47%)	5.16% (11.17%)

Table 10: Composition of News Classes with Different Thresholds on WESS Scores

r	Num Negative	Num Neutral	Num Positive
0	46.54% (100.00%)	9.06% (100.00%)	44.40% (100.00%)
0.3	42.85% (92.08%)	13.99% (154.43%)	43.16% (97.19%)
1	39.25% (84.33%)	20.32% (224.32%)	40.43% (91.06%)
3	31.12% (66.87%)	34.62% (382.22%)	34.25% (77.14%)
5	25.24% (54.24%)	46.49% (513.20%)	28.27% (63.66%)
10	17.51% (37.64%)	61.39% (677.67%)	21.10% (47.52%)
15	9.83% (21.13%)	77.68% (857.58%)	12.48% (28.11%)
20	7.98% (17.15%)	84.63% (934.20%)	7.39% (16.65%)
25	4.22% (9.06%)	91.95% (1015.06%)	3.83% (8.63%)

3.6 Case Studies

3.6.1 November 30, 2016: Postive Spike

The first case study investigates the event of an expected production cut by OPEC. On the 30th of November, 2016. Reports concerning this shock were considered as positive news for crude oil price since upcoming negative supply shock generally leads to expectation on soaring prices.

Figure 18: Crude Oil Price and Number of Events within 10 Days

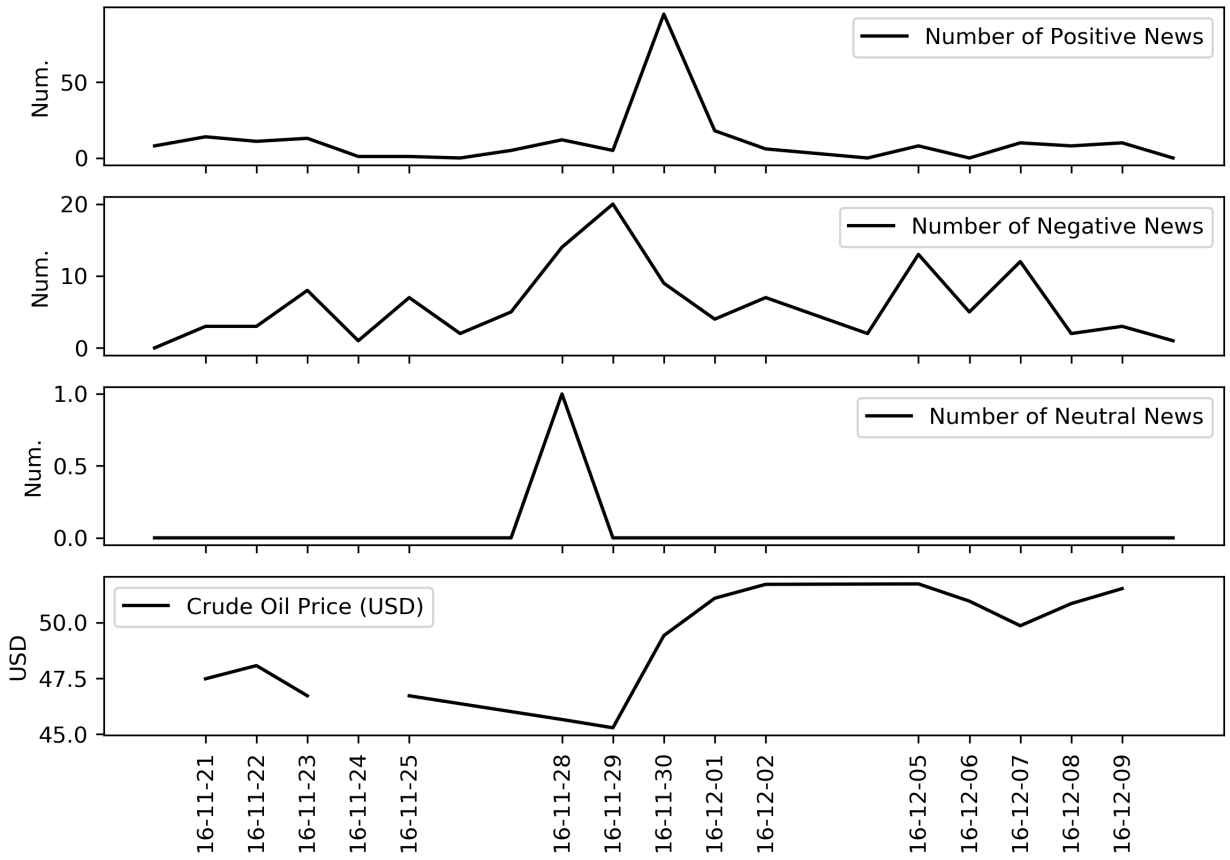

3.6.2 December 6, 2018: Negative Spike

The US had become a net oil-exporting country in the week of Dec. 6, for the first time in 75 years (citation: Bloomberg). This major shift marks a potential negative shock in the demand side of the crude oil market and news reporting this fact was all considered as negative events for the crude oil price.

Figure 19: Crude Oil Price and Number of Events within 10 Days

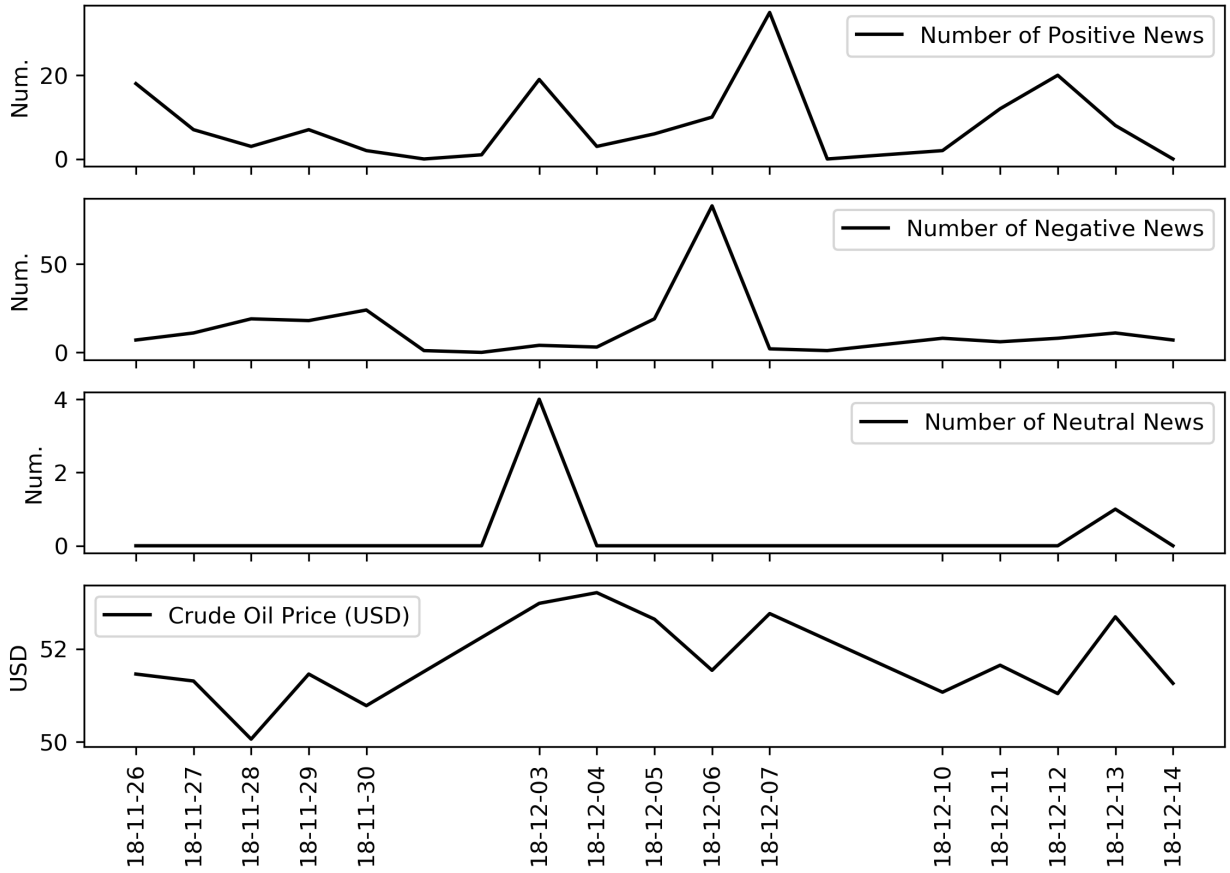

3.6.3 June 12∼13, 2019: Positive Spike in Down Period

Unlike in the two previous cases, the third case investigates the impact of positive news spike in a period with falling oil prices. Table and Table in the appendix include more complete lists of news about crude oil published on Bloomberg on June 12 and 13, 2019.

The crude oil price had been decreasing since April 2019. The tension between the US and Iran had been accumulating since the US withdrew from the Joint Comprehensive Plan of Action on the 8th of May and alleged Iran for the first Gulf of Oman incident occurred on the 12th. In response, Iran had threatened to close the Strait of Hormuz, which is an important channel for international oil shipping. However, as we can see from the Figure 20, before Jun. 12, the major theme of news available was positive, this can be explained by the stable oil supply from Saudi Arabia and other oil-exporting countries.

The story changed on Jun. 13, when the second Gulf of Oman incident happened. Two oil

tankers were attacked while passing the Gulf of Oman, which further escalated the tension between the US and Iran, and the market had sufficient reason to expect a negative supply shock. With the arrival of such a cluster of positive news (positive for crude oil prices), the price increased significantly after the incident but returned to its normal decreasing trend after approximately one week.

Figure 20: Crude Oil Price and Number of Events within 10 Days

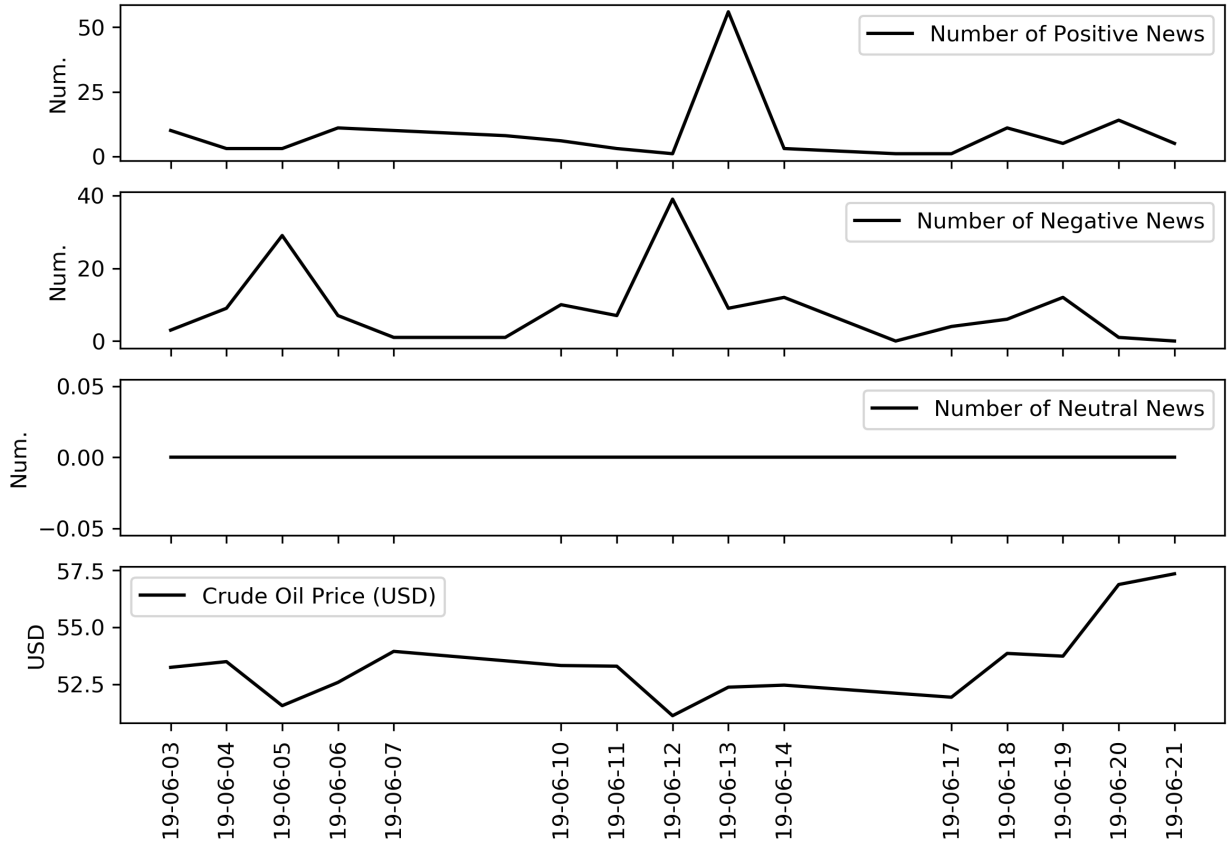

4 Model

4.1 Framework: An Intuitive Explanation with Example

Figure 21 illustrates the framework of our model as a directed acyclic graph (DAG). In a DAG, an arrow $X \to Y$ indicates that X is causing Y so that the realization of variable Y depends on X.

On each day t, the state of world is denoted as ω_t, which is a high dimensional variable describing everything happening in the world on day t.

The first component in this model consists of a batch of news subscriptions to various news sources. Each of these news sources summarize ω_t as a collection of news articles, which are literally a collection of texts. Some sources provide summary on these articles as well as analysis on the potential economic impacts from events mentioned in these articles. We define the collection of news articles altogether with any summary and analysis from the news provider to be the information flow (conditioned on subscriptions). For example, consider one trader who only read Wall Street Journal in his office everyday, then his perception of the state of world is formed by (therefore, a function of) those news articles and analysis of news on Wall Street Journal. In this case all those articles and analysis is precisely the information flow received by this trader.

Given an arbitrary time period, say one day, the information flow within this period is simply the collection of news reported within this time period. We denote the information flow on day t as IF_t. Therefore, IF_t provides a summary of ω_t just like one can learn the state of world from reading news paper articles.

The information flow consists of texts and summaries of news articles, one needs to quantify the information flow before applying quantitative models to it. This paper works on predicting future returns, and predictive models such as neural networks are expecting quantitative inputs (e.g., real-valued vectors) instead of qualitative inputs (e.g., plain texts and headlines of articles). Therefore, we would need to quantify the abstract information flow on each day t as a real-valued vector, $\mathbf{x}_t$. Ideally, $\mathbf{x}_t$ should provide a finer summary, especially sentiments, of the IF_t as well as ω_t. Sometime we refer to $\mathbf{x}$ as the quantified information flow and IF as the abstract information flow.

The last component is the realized return r_t. The true state ω_t is determining the actual realized return r_t on day t. Moreover, since traders are often reacting to news reports, so the quantified information flow $\mathbf{x}_t$ affects r_t as well.

For example, imagine there is an undergraduate student interested in crude oil market. Due to his limited budget, he has subscriptions to Wall Street Journal and the Economist only. For simplicity, assume he stays in his office the whole day and does not absorb any

finance-related news from other sources. One day, denoted day t, OPEC announces a cut in oil export during a conference, this conference and announcement contribute to ω_t. Shortly after the announcement is made, both WSJ and the Economist report this export restriction and these news articles published describe ω_t and constitute the information flow IF_t of this student. Note that IF_t depends on and reflects ω_t but it is only a qualitative proxy since IF_t is essentially a batch of news articles. If this student wishes to build a predictive model for r_{t+1} based information flow he receives, IF_t must be quantified. One simplest way of quantifying information flows is to manually assign each article a sentiment score: he could assign 10 (-10) scores to all articles describing events could increase (decrease) oil returns. Then taking the average score of all articles in IF_t gives a real-number $\mathbf{x}_t$, which is a quantitative representation of IF_t.

4.2 Formal Framework

This section is devoted to revise the proposed framework but using a more formal mathematical language. Recall that Figure 21 illustrates the framework of the proposed framework.

4.2.1 Timestamps

In the following discussion, this paper uses non-negative real numbers, $t \in \mathbb{R}_+$, to indicate timestamps accurate to seconds. Specifically, 12 am of first day in dataset (January 3, 2000) corresponds to $t = 0$ and the length of 24 hours is normalized to one. Using this timestamp convention, an integer t indicates the beginning of the t^{th} trading day in the dataset. For example, the time stamp $t = 10$ represents 12:00 am of the 10^{th} trading day in our dataset, which was January 18, 2000. Similarly, $t = 10 + \frac{10}{24}$ denotes 10:00 am of January 18, 2000.

Each news article in the dataset has one timestamp τ corresponding to the time when this piece of news is published. Because this paper works on a daily basis prediction task, we need to discretize the continuous timestamp of t into integers and convert the frequency into daily frequency.

Figure 21: The Framework

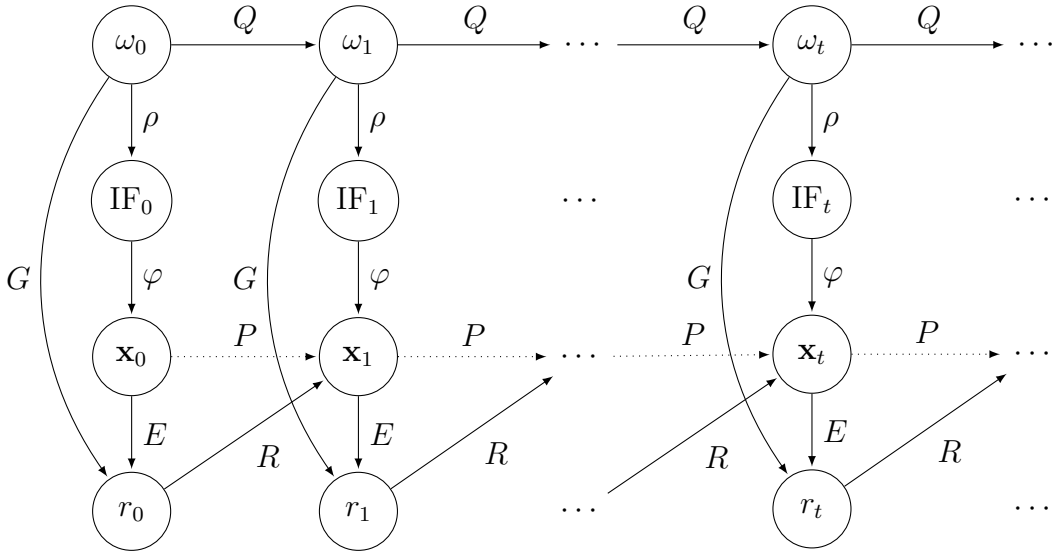

4.2.2 States of World

On each day $t \in \mathbb{Z}_+$, the real state of world is denoted as $\omega_t \in \Omega$, which is a latent variable describing everything happening in the world on day t. The latent of possible states of world Ω is left unspecified because we do not need to interpret ω_t explicitly for this prediction task.

The dynamics of $\{\omega_t\}$ is a stochastic process governed a transition probability Q. The process evolves following equation (4.1):

$$\omega_t \sim Q(\omega_t | \omega_{t-1}, \omega_{t-2}, \cdots, \omega_0) \tag{4.1}$$

4.2.3 Information Flow

The first component in this model consists of a batch of news subscriptions to various news sources. Each of these news sources summarize ω_t as a collection of news articles, which are literally a collection of texts. Some sources provide summary on these articles as well as analysis on the potential economic impacts from events mentioned in these articles. We define the collection of news articles altogether with any summary and analysis from the news provider to be the **information flow** (conditioned on subscriptions), denoted as $\rho(\omega_t)$. The functional form suggests the information flow received by an individual depends

on both the state of world ω_t and another subscription function ρ characterizing how many resources this individual has access to. One individual with subscription function ρ_1 has access to more resources than another one with ρ_2 if

$$\rho_2(\omega) \subseteq \rho_1(\omega) \quad \forall \omega \in \Omega \tag{4.2}$$

For example, consider one trader who only read Wall Street Journal in his office everyday, then his perception of the state of world is formed by (therefore, a function of) those news articles and analysis of news on Wall Street Journal. In this case all those articles and analysis is precisely the information flow received by this trader.

For an arbitrary time period, say one day, the information flow within this period is simply the collection of news reported within this time period. We denote the information flow on day t as IF_t. Therefore, $\text{IF}_t(\omega_t)$ provides a summary of ω_t.

In this study, our subscription function ρ is defined by the RPNA dataset, which consists of four sources: Dow Jones Newswires, Wall Street Journal, Barron's, and MarketWatch. So the information flow used in this paper is the collection of news articles and relevant analysis from the above-mentioned four sources.

Formally, let $N = 106,960$ denote total number of news articles about crude oils [4] in the RPNA dataset over the considered period from January 1, 2000 to October 31, 2019. One may firstly sort all N news based on the timestamp when each news arrived. Then each piece of news in the dataset can be uniquely indexed using an integer $n \in \{1, 2, \cdots, N\}$. For example, news article n is the n^{th} news in the dataset. Let τ_n denote the time when the n^{th} news article was reported.

Using this indexing method, news arrive within a time period $\mathcal{T}$ can be presented as a set of integers $\theta_{\mathcal{T}}$. Therefore, since $[t, t+1)$ is precisely the period of 24 hours on day t, $\theta_{[t,t+1)}$ denotes the set of integer indices of news published on day t. Because each piece of news has a unique integer index, instead of a set of news articles, the information flow can be equivalently defined as the set of indices of these news articles. Hence, this paper defines the **information flow on day** t, IF_t, to be the set of indices of news articles in the dataset

[4] Recall that RPNA dataset includes a topic for each article, the topic of article is identified based on the headline, keywords and body text of the news article.

that are published on day t:

$$\mathrm{IF}_t = \left\{ n : n \in \theta_{[t,t+1)} \right\} \tag{4.3}$$

Figure 22 summarizes the workflow of the prediction task in a minimal setting: predicting r_{t+1} using information on the day t only. On the timeline, each of t, $t+1$ and $t+2$ denotes the beginning of the day, p_t and p_{t+1} indicate the time when the closing price is computed. At the beginning of day $t+1$, say 1 a.m., the prediction task task is to predict the return r_{t+1} of day $t+1$ from both p_t and IF_t using a predictive model. Let $\hat{r}_{t+1}(p_t, \mathrm{IF}_t)$ denote the prediction for r_{t+1}, and traders may design their trading strategy on day $t+1$ based on this prediction. Later when the market closes in the afternoon of day $t+1$ and p_{t+1} is realized. The real return r_{t+1} can be computed from p_{t+1} and p_t using equation (3.1). Comparing $\hat{r}_{t+1}$ and r_{t+1} can evaluate the predictive power of the model used.

Figure 22: Workflow of the Prediction Task

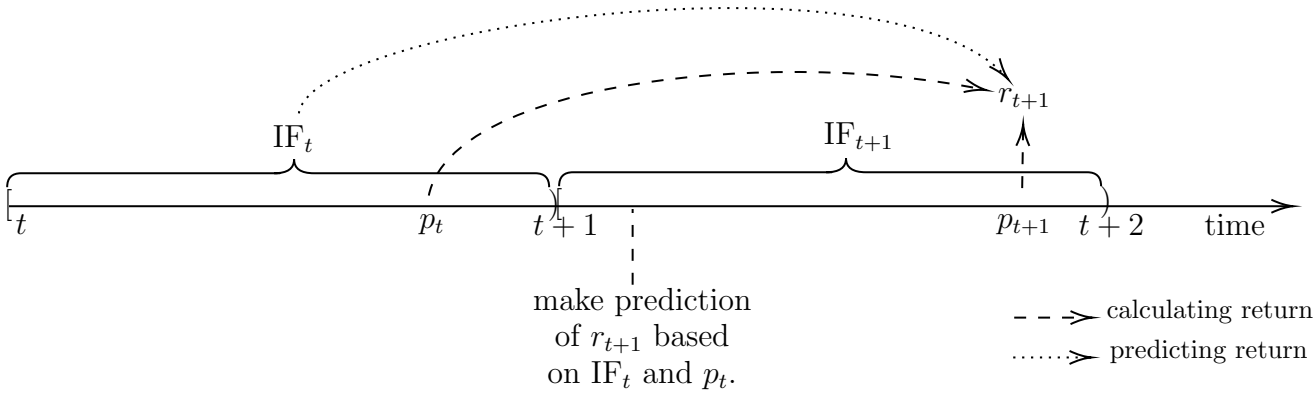

4.2.4 Characteristic Function

In this paper, we are approaching the prediction task using auto-regressive models, which means we are using lagged values to predict the future. Let $\mathcal{M}$ denote a predictive model uses information in the past to the future crude oil return.

For instance, if one is building a model conducting one step ahead forecasting based on historical information (both information flow of past days and historical returns) up to ℓ

days in the past, $\mathcal{M}$ is a map from information in the past ℓ days to a prediction:

$$\mathcal{M}\left(\begin{bmatrix}\text{IF}_{t-\ell+1}\\ r_{t-\ell+1}\end{bmatrix}, \begin{bmatrix}\text{IF}_{t-\ell+2}\\ r_{t-\ell+2}\end{bmatrix}, \cdots, \begin{bmatrix}\text{IF}_{t}\\ r_{t}\end{bmatrix}\right) = \hat{r}_{t+1} \tag{4.4}$$

Then the model $\mathcal{M}$ is evaluated based on how close r_{t+1} and $\hat{r}_{t+1}$ are. However, each information flow IF_t is a set of (indices of) news articles, these indices remain abstract and do not have any meaning on themselves. Simply feeding these indices to a machine learning model will not generate any meaningful result, one needs to extract some features from those news articles for predictive models. In order to quantify these abstract information flow, we propose a mapping called characteristic function. Let $\mathcal{T}$ be an arbitrary time period, such as the whole day t:

$$\mathcal{T} := [t, t+1) \tag{4.5}$$

We define a characteristic function φ [5] as a mapping from a time period $\mathcal{T}$ to a real-valued vector $\varphi(\mathcal{T}) \in \mathbb{R}^d$, where d denotes the number of features constructed. Ideally, $\varphi(\mathcal{T})$ should provide a quantitative summary from various aspects of news articles in $\text{IF}_{\mathcal{T}}$.

For example, one valid characteristic function φ can construct the following two features: 1) the the number of news articles (events) in period $\mathcal{T}$ and 2) the average event sentiment score of these news:

$$\varphi(\mathcal{T}) = \begin{bmatrix} |\{n : \tau_n \in \mathcal{T}\}| \\ \frac{1}{|\{n:\tau_n \in \mathcal{T}\}|} \sum_{n \ s.t. \tau_n \in \mathcal{T}} \text{ESS}_n \end{bmatrix} = \begin{bmatrix} \text{Number of News on Day } t \\ \text{Average ESS Score of News on Day } t \end{bmatrix} \in \mathbb{R}^2 \tag{4.6}$$

Note that in subsequent sections, the characteristic function actually used has far more features than the example in equation (4.6).

With a chosen characteristic function φ, one can quantify the qualitative information flow

[5] In the context of probability, the characteristic function of a distribution fully describes the distribution, refer to (Ushakov 1999) for a review of this topic. Here we define the characteristic function to be the function mapping a collection of news to a vector $\mathbf{x}$ of summary statistic of these news.

on each day t using a real-valued vector $\mathbf{x}_t$:

$$\mathbf{x}_t := \varphi([t, t+1)) \tag{4.7}$$

Note that $\mathbf{x}_t$ can be constructed only after day t ends, that is, at the beginning of day $t+1$. After the prediction of r_{t+1} is made using $\mathbf{x}_t$ (and p_t as well), one may design and modify trading strategy used on day $t+1$ based on the prediction of r_{t+1}. All of these things happen at the beginning of day $t+1$ before the market opens.

The complete workflow of forecasting and model evaluation can be summarized as

(i) (At the beginning of day $t+1$) gather all news articles published on and returns of previous days: $\text{IF}_{t-\ell}$, ..., IF_t and $r_{t-\ell}$, ..., r_t.

(ii) (At the beginning of day $t+1$) quantify news articles gathered in the previous step into $\mathbf{x}_{t-\ell}$, ..., $\mathbf{x}_t$.

(iii) (At the beginning of day $t+1$) plug $r_{t-\ell}$, ..., r_t and $\mathbf{x}_{t-\ell}$, ..., $\mathbf{x}_t$ into a predictive model $\mathcal{M}$ to generate prediction $\hat{r}_{t+1}$.

(iv) (While market is opening on day $t+1$) trade based on the prediction $\hat{r}_{t+1}$.

(v) (When market closes on day $t+1$) compute the actual return r_{t+1} using p_t and p_{t+1}.

(vi) (When market closes on day $t+1$) assess the performance of $\mathcal{M}$ by comparing r_{t+1} and $\hat{r}_{t+1}$. Note that the model's performance can also be evaluated based on the profit made this day.

(vii) Move to day $t+1$ and repeat the whole process.

In this paper, the characteristic function used provides a summary on the sentiment scores provided by RPNA dataset, therefore, we define $\mathbf{x}_t$ to be the **sentiment** of the information flow on day t.

Using characteristic functions, the predictive model in equation (4.4) can be equivalently

expressed as

$$\mathcal{M}\left(\begin{bmatrix}\varphi([t-\ell+1,t-\ell+2))\\ r_{t-\ell+1}\end{bmatrix},\begin{bmatrix}\varphi([t-\ell+2,t-\ell+3))\\ r_{t-\ell+2}\end{bmatrix},\cdots,\begin{bmatrix}\varphi([t,t+1))\\ r_{t}\end{bmatrix}\right) \tag{4.8}$$

$$=\mathcal{M}\left(\mathbf{x}_{t-\ell+1},r_{t-\ell+1},\mathbf{x}_{t-\ell+2},r_{t-\ell+2},\cdots,\mathbf{x}_t,r_t\right)=\hat{r}_{t+1} \tag{4.9}$$

Gathering First or Summarizing First Exchanging the order of applying characteristic function and aggregating information induces subtle difference in the model. Note that we may aggregate information flow first , that is, take $\mathcal{T}'=[t-\ell+1,t+1)$. Then, we can construct a summary of all news arrive in the past ℓ days by applying φ on $\mathcal{T}'$:

$$\mathbf{x}_{t-\ell+1:t}=\varphi(\mathcal{T}') \tag{4.10}$$

Hence, $\mathbf{x}_{t-\ell+1:t}$ is a quantitative summary of all news arrive from day $t-\ell+1$ to day t. Using this notation, the following alternative formulation is equally valid,

$$\mathcal{M}\left(\varphi([t-\ell+1,t+1)),r_{t-\ell+1},r_{r-\ell+2},\cdots,r_t\right) \tag{4.11}$$

$$=\mathcal{M}\left(\mathbf{x}_{t-\ell+1:t},r_{t-\ell+1},r_{r-\ell+2},\cdots,r_t\right)=\hat{r}_{t+1} \tag{4.12}$$

In the following parts of this paper, we call equation (4.9) the **summarizing-first** formulation since it apply φ on news arrived in each day first, then feeds the collection of summaries to a predictive model. And, we call (4.12) the **gathering-first** formulation, since it firstly collects all news arrive in the time period of consideration, and apply the characteristic function on all these news.

There is a trade-off between choosing which formulation to use. For example, when $\ell=10$, the summarizing-first paradigm generates one feature vector $\mathbf{x}$ for each of the past 10 days of consideration. In total, the 10 feature vectors generated contains $10d$ real values, where d is the dimension of φ's codomain. However, suppose $\mathbf{x}$ contains mean and standard deviation of ESS scores, each $\mathbf{x}$ is only built from a few news arrive within one single day and information contained in $\mathbf{x}$ could be biased. In contrast, the feature vector constructed using the gathering-first approach is built from much more news articles and can reflect the state

of world more accurately as a result. The drawback of using the gathering-first formulation is that it generates too few features: no matter how large the scope ℓ is, the gathering-first approach only constructs one feature vector $\mathbf{x}$, which contains d real values.

To fully leverage information from the news articles, predictive models used in this paper forecast returns based on features constructed using both paradigms: the model is forecasting the future return r_{t+1} using ℓ daily summary feature vectors and one aggregate summary feature vector.

4.2.5 Inter-temporal Dependency

The state of world is changing from ω_t to ω_{t+1} between two consecutive trading days, and ω_{t+1} depends on ω_t. Moreover, $\mathbf{x}_t$ affects $\mathbf{x}_{t+1}$ as well since certain type of events are reported continuously for more than one day, and the news sentiments exhibits inter-temporal correlation. For example, export restrictions by OPEC countries is a negative news for crude oil prices. An article about this OPEC meeting is reported on the first day and an analysis report of this restriction is published on the second day.

Lastly, some news on day $t+1$ are simply reporting the return on the previous day so that r_t impacts $\mathbf{x}_{t+1}$ as well.

4.3 Empirical Model

The empirical models to be estimated in this paper are focusing on the dynamics of sentiments $\{\mathbf{x}_t\}_t$ and returns $\{r_t\}_t$.

As examined in the data section, the inter-temporal correlation among returns is weak, hence, predicting current r_t using lagged value of returns is far too challenging for simple models. The framework proposed by this paper aims to use series of sentiments $\{\mathbf{x}_t\}_t$ constructed, which have stronger inter-temporal correlation, to bridge the gap.

Specifically, in Figure 21, each pair of $\mathbf{x}_t$ and $\mathbf{x}_{t+1}$ are correlation through the chain $\mathbf{x}_t \to \omega_t \to \omega_{t+1} \to \mathbf{x}_{t+1}$. Therefore, in order to model the dynamic from $\mathbf{x}_t$ to $\mathbf{x}_{t+1}$, we have to construct models estimating P, E, and R in the graph first.

Figure 23 illustrates the idea of forecasting returns via sentiments. Suppose we wish to

predict returns r_t on day t using only information at time $t-\ell$ (i.e., both $r_{t-\ell}$ and $\mathbf{x}_{t-\ell}$) for some integer $\ell > 1$. The ACF and PACF of return series have only a few significant lags, so that the arrow from $r_{t-\ell}$ to r_t is blocked by this weak correlation. This prevents one from forecasting r_t using $r_{t-\ell}$ with directly a simple model like autoregression integrated moving average (ARIMA). However, the strong inter-temporal correlation in sentiment series allows one to predict Sentiment_t using $\text{Sentiment}_{t-\ell}$. Secondly, the correlation between sentiment and return enables the model to estimate r_t from the prediction of Sentiment_t. The composite of two steps above provides an indirect approach of forecasting r_t using information at time $t-\ell$.

Figure 23: Framework

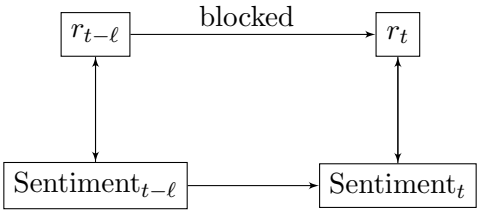

Literature have been using hidden Markov models (HMMs) for time series forecasting. As mentioned before, $\mathbf{x}_{t+1}$ are determined by the collection of news on day $t+1$ (the information flow) via a characteristic function. However, many of those news in IF_{t+1} are simply reporting past price movements of crude oil, that is, r_t. Therefore, the proposed framework extends the hidden Markov framework by allowing the directed edge from r_t to $\mathbf{x}_{t+1}$, the edge R, to explicitly model the impact of historical price movements on future news sentiment.

We model $\{\mathbf{x}_t\}_t$ as a stochastic process whose dynamics is governed by the **transition probability**, P, and the **reporting probability**, R, plus random noises:

$$\mathbf{x}_t = \mathbf{x}_t^A + \mathbf{x}_t^B + \varepsilon_t \tag{4.13}$$

$$\text{where} \quad \mathbf{x}_t^A \sim P(\mathbf{x}_t^A | \mathbf{x}_{t-1}) \tag{4.14}$$

$$\mathbf{x}_t^B \sim R(\mathbf{x}_t^A | r_{t-1}) \tag{4.15}$$

The transition probability P models the impact of past news sentiments on the future news sentiment, and $\mathbf{x}_t^A$ is the portion of sentiment $\mathbf{x}_t$ solely determined by the inter-temporal

correlation among $\mathbf{x}$. In addition, another reporting probability R models the impact of past returns on future news sentiment. Hence, $\mathbf{x}_t^B$ is the part of $\mathbf{x}_t$ responses to past price movement. For example, $\mathbf{x}_t^B$ could be the average of sentiment scores assigned to articles simply reporting the return on the previous day. More generally, two parts of news sentiments can be merged using one joint distribution PR:

$$\mathbf{x}_t \sim PR(\mathbf{x}_t|\mathbf{x}_{t-1}, r_{t-1}) \tag{4.16}$$

Expanding equation (4.16) recursively shows that $\mathbf{x}_t$ is in fact impacted by all historical values of $\mathbf{x}_t$ and r_t. Therefore, the entire history of $\{\mathbf{x}_{t-1}, \mathbf{x}_{t-2}, \cdots, \mathbf{x}_0\}$ and $\{r_{t-1}, r_{t-2}, \cdots, r_0\}$ contribute to the distribution of $\mathbf{x}_t$

$$\mathbf{x}_t \sim F(\mathbf{x}_t|\mathbf{x}_{t-1}, \mathbf{x}_{t-2}, \cdots, \mathbf{x}_0, r_{t-1}, r_{t-2}, \cdots, r_0) \tag{4.17}$$

The **order** of a Markov model determines the length of its memory, a Markov model has order ℓ if the distribution of an arbitrary random variable Y_t only depends on the past ℓ values, that is, for every $t > \ell$,

$$P(Y_t|Y_{t-1}, Y_{t-2}, \cdots, Y_0) = P(Y_t|Y_{t-1}, Y_{t-2}, \cdots, Y_{t-\ell}) \tag{4.18}$$

In most cases, the impact of observations in the distant past, say $\mathbf{x}_{t-1,000}$, on the current observation $\mathbf{x}_t$ is negligible. Therefore, for simplicity, we assume the chain in equation (4.17) is assumed to have a finite order ℓ. Hence,

$$\mathbf{x}_t \sim F(\mathbf{x}_t|\mathbf{x}_{t-1}, \mathbf{x}_{t-2}, \cdots, \mathbf{x}_{t-\ell}, r_{t-1}, r_{t-2}, \cdots, r_{t-\ell}) \tag{4.19}$$

As mentioned before, the actual return r_t is determined by multiple factors. Firstly, all those events happening on day t, that is, ω_t affects r_t. Moreover, traders are often trade according to news articles ($\mathbf{x}_t$) they have read, and traders' behaviours affects the market and therefore r_t. Hence, $\mathbf{x}_t$ is affecting r_t indirectly via traders' behaviours as well. The

distribution of r_t follows distribution E termed **emission probability**. [6] In particular, E maps the current state of world ω_t and current news sentiment $\mathbf{x}_t$ to a distribution of realized returns r_t. Hence, the distribution of r_t depends on both the true state of world and the news sentiment.

$$r_t \sim E(r|\omega_t, \mathbf{x}_t, r_{t-1}, r_{t-2}, \cdots, r_{t-\ell}) \tag{4.20}$$

For generality, even not shown in Figure 21, we assume the distribution of r_t depends on historical returns too. Therefore, the distribution in equation (4.20) includes the lagged values of returns as well. However the impact of adding historical returns should be insignificant given previous analysis on autocorrelations. Moreover, since we assume the Markov chain of returns has order ℓ, so that historical return values before $r - \ell$ are discarded.

Note that the series of $\{\omega_t\}$ is latent, the model has only observations on $\{\mathbf{x}_t\}$ and $\{r_t\}$. For each day t, we can now construct two predictors of return, r_t,

$$\hat{r}_t^{\text{raw}} = \mathbb{E}[r_t|r_{t-1}, r_{t-2}, \cdots, r_{t-\ell}] \tag{4.21}$$

$$= \mathcal{M}^{\text{raw}}(r_{t-1}, r_{t-2}, \cdots, r_{t-\ell}) \tag{4.22}$$

$$\hat{r}_t^{\text{senti}} = \mathbb{E}[r_t|\mathbf{x}_{t-1}, \mathbf{x}_{t-2}, \cdots, \mathbf{x}_{t-\ell}, r_{t-1}, r_{t-2}, \cdots, r_{t-\ell}] \tag{4.23}$$

$$= \mathcal{M}^{\text{senti}}(\mathbf{x}_{t-1}, \mathbf{x}_{t-2}, \cdots, \mathbf{x}_{t-\ell}, r_{t-1}, r_{t-2}, \cdots, r_{t-\ell}) \tag{4.24}$$

The first model $\mathcal{M}^{\text{raw}}$ is predicting the return following a classical auto-regressive manner, that is, using lagged values of return only. In contrast, the second model $\mathcal{M}^{\text{senti}}$ incorporates the sentiment series as well.

Using this framework, we may formulate the original question of interest as whether $\hat{r}_t^{\text{senti}}$ is a significantly better prediction of r_{t+1} than $\hat{r}_t^{\text{raw}}$, in terms of prediction accuracy. Recall the workflow in Figure 22, since the closing price p_t is realized near the end of day and the return r_t can be computed at the same time. Based on Figure 13, most information within IF_t will arrive before r_t is realized, if the market is efficient, a great portion of IF_t should have already been reflected in r_t. In this case, IF_t, and therefore $\mathbf{x}_t$, will not provide

[6] In this paper, E is a specific distribution and $\mathbb{E}$ denotes the expectation operator.

meaningful information to the prediction of r_t. Therefore, if the efficient market hypothesis holds true, the performance of two above-mentioned predictions should be similar. And we can conclude that adding the news sentiment series does not help predict returns. In contrast, if $\hat{r}_t^{\text{senti}}$ outperformed $\hat{r}_t^{\text{raw}}$ a lot, then we can claim that the news sentiment series is capable of improving return predictions.

In experiment section of this paper, this paper uses different types of statistical learning models to estimate $\hat{r}_t^{\text{raw}}$ and $\hat{r}_t^{\text{senti}}$, then compare their performances.

5 Experiments

5.1 Procedures

The empirical model in section 4.3 gives a brief description on how to assess the predictive power of models with and without sentiment dataset. We need to choose a specific characteristic function φ and predictive model $\mathcal{M}$ in order to generate quantitive metrics and compare performances.

5.1.1 Feature Constructions

The previous section described the rough idea of using a characteristic function to quantify an information flow. Before implementing any statistical model, the first step is to choose a specific characteristic function which extracts quantitive summary statistics from a given information flow. In order to maximize the number of features extracted, the proposed characteristic function utilizes features from both the gathering first and summarizing first paradigms.

Let $\ell \in \mathbb{Z}_+$ denote the length of model's memory. That is, while predicting r_t, the model can only use information from day $t-\ell$ to day $t-1$. This paper chooses $\ell = 31$ so that the model uses information within a whole month to predict one return.

Firstly, for each day from day $t-\ell$ to day $t-1$, the characteristic function computes all variables in Table 11. Even though `NUM_EVENTS` can be deduced from `ESS_MEAN` and `ESS_TOTAL`, we decided to include it as a proxy of the volatility of news networks.

Table 11: Daily Summary Statistics from Summarizing-First Paradigm (1)

Code Name	Variable	Code Name	Variable
ESS_MEAN	Average ESS	WESS_MEAN	Average WESS
ESS_TOTAL	Sum of ESS	WESS_TOTAL	Sum of WESS
NUM_EVENTS	Number of Events		

Moreover, following the methodology in section 3.5, the characteristic function classifies positive (negative / neutral) news using their ESS (WESS) scores and a predefined threshold r. The characteristic function added the number of news in each class to the daily summary.

Table 12: Daily Summary Statistics from Summarizing-First Paradigm (2)

Code Name	Variable	Code Name	Variable
NUM_POSITIVE_ESS	# news s.t. ESS $> r$	NUM_POSITIVE_WESS	# news s.t. WESS $> r$
NUM_NEGATIVE_ESS	# news s.t. ESS $< -r$	NUM_NEGATIVE_WESS	# news s.t. WESS $< -r$
NUM_NEUTRAL_ESS	# news s.t. ESS $\in [-r, r]$	NUM_NEUTRAL_WESS	# news s.t. WESS $\in [-r, r]$

Table 11 and Table 12 together provide the daily summary for the sentiment dataset from day $t - \ell$ to day $t - 1$, and concatenating them gives 11ℓ features in total. We denote the characteristic function computing daily summary as φ_{daily}, for a given information flow on day t, $\varphi_{\text{daily}}(\text{IF}_t)$ calculates 11 summary statistics of IF_t.

Studies on the gold future market suggests that negative news sentiments tend to invoke greater responses from the market (Smales 2014). It is likely for this observation to be true in crude oil market as well since gold market and crude oil market share many similar features. One way to separate impacts from positive and negative news is to split all news into a positive and a negative group (neutral news are dropped). Then, applying φ_{daily} on these two subsets of information flow gives two copies of summaries, one for positive news and one for negative news. However, distinguishing positive and negative news while constructing daily summary doubles the number of features generated (from 11ℓ to 22ℓ), and can potentially lead to the curse of dimensionality especially when ℓ is large (Friedman 1997). Therefore, for the daily summary, the proposed characteristic function only counts the number of news in each class but does not calculate detailed summary statistics (e.g., standard deviation and percentiles).

In contrast, while processing the aggregated information flow in the period of consideration, $\text{IF}_{[t-\ell,t)}$ (i.e., all news from day $t-\ell$ to day $t-1$), instead of creating ℓ copies of daily summaries for ℓ days, the number of features constructed no longer depends on ℓ. This allows us to choose more complicated characteristic function for the aggregate information flow. Therefore, we may choose a characteristic function distinguishing positive and negative news and computes more detailed summary statistics.

Let $\varphi_{\text{aggregate}}$ denote the second characteristic function extracting features from $\text{IF}_{[t-\ell,t)}$. Table 13 enumerates 8 types of summary statistics used. Firstly, $\varphi_{\text{aggregate}}$ computes the 8 statistics in Table 13 for ESS and WESS of all news in $\text{IF}_{[t-\ell,t)}$ (16 features in total).

Table 13: Summary Statistics from Gathering-First Paradigm (1)

Code Name	Variable
`x_count`	Number of Samples X
`x_mean`	Average of X
`x_std`	Standard Deviation
`x_min`	Minimum
`x_25%`	25^{th} Percentile
`x_50%`	Median
`x_75%`	75^{th} Percentile
`x_max`	Maximum

To emphasize extreme events more, we then compute the 8 summary statistics in Table 13 for the squared ESS and WESS scores as well (16 features in total). Note that ESS and WESS scores range from -50 to 50, the squared scores are defined following equation (5.1) so that their signs are preserved.

$$\begin{aligned} \text{ESS}^2 &:= \text{sign}(\text{ESS}) \times \text{ESS}^2 \\ \text{WESS}^2 &:= \text{sign}(\text{WESS}) \times \text{WESS}^2 \end{aligned} \tag{5.1}$$

Afterwards, we split $\text{IF}_{[t-\ell,t)}$ into the positive group, $\text{IF}^{+}_{[t-\ell,t)}$, and the negative group, $\text{IF}^{-}_{[t-\ell,t)}$, according to the sign of each news' ESS score (news with zero ESS score are discarded). Note that by the definition of WESS, signs of ESS and WESS are always the same, hence, splitting $\text{IF}_{[t-\ell,t)}$ based on ESS and WESS always gives the same outcome. Then, $\varphi_{\text{aggregate}}$ summarizes

the number of news, the average ESS and the average WESS for each of $\text{IF}^{+}_{[t-\ell,t)}$ and $\text{IF}^{-}_{[t-\ell,t)}$ (6 features in total).

Lastly, as we noticed in the data exploration, there are two clusters of ESS scores (at -15 and 18). Moreover, news article assigned with these two values of ESS scores are in general reports of past price movements and carry little information about future price changes. To address this issue, we define $\text{IF}^{++}_{[t-\ell,t)}$ (extremely positive news) to be the subset of $\text{IF}_{[t-\ell,t)}$ with ESS strictly greater than 18, and $\text{IF}^{--}_{[t-\ell,t)}$ (extremely negative news) to be these news with ESS strictly less than -15. Afterwards, $\varphi_{\text{aggregate}}$ summarizes the number of extremely positive (negative), the average ESS and the average WESS of news in $\text{IF}^{++}_{[t-\ell,t)}$ and $\text{IF}^{--}_{[t-\ell,t)}$ (6 features in total).

Overall, $\varphi_{\text{aggregate}}$ constructs 44 features to summarize each information flow $\text{IF}_{[t-\ell,t)}$. Altogether with the 11ℓ features from φ_{daily}, $11\ell + 44$ features are used to predict the return r_t. For example, there would be 385 features if one chose ℓ to be 31. Given there are around 5,000 daily returns to train the model, using approximate 400 independent variable is reasonable.

5.1.2 Rolling-Window Method

The second step of the pipeline is to construct a batch of feature-target pairs (called a sample), (X_t, r_t), so that we can evaluate model $\mathcal{M}$ based on how close $\mathcal{M}(X_t)$ and r_t are. Let $\ell = 31$ for now, returns in the first month are discarded from the dataset since we do not have sufficient number of days to construct these features required. Afterwards, a rolling-window method generates a training set from the series of returns and news dataset as illustrated in Figure 24.

Figure 24: Using Rolling Window to Construct (X_t, r_t) pairs

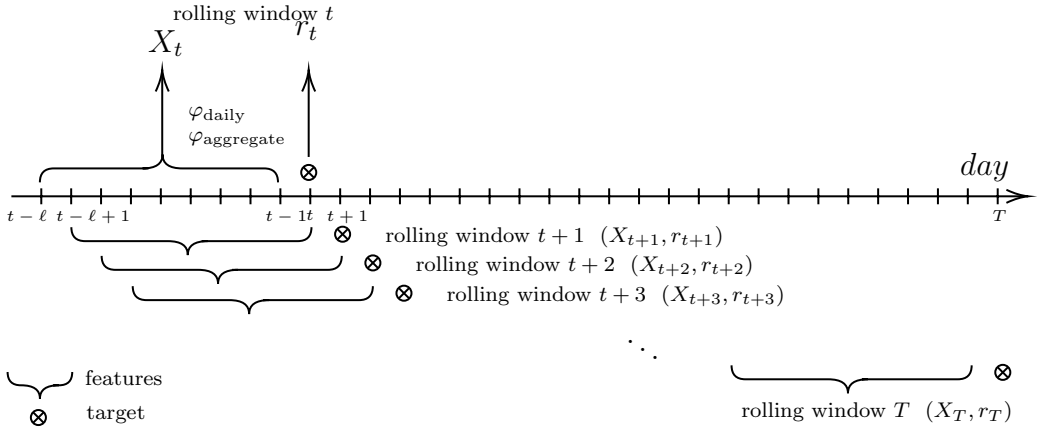

For each day t with valid return r_t (those days with missing returns are discarded), the set of features X_t consists of 31 daily summary from φ_{daily}, one aggregate summary from $\varphi_{\text{aggregate}}$ and 31 lagged values of returns.

$$X_t^{\ell=31} := \left\{\varphi_{\text{daily}}(\text{IF}_{t-31}), \cdots, \varphi_{\text{daily}}(\text{IF}_{t-1}), \varphi_{\text{aggregate}}(\text{IF}_{[t-31,t)}), r_{t-31}, \cdots, r_{t-1}\right\} \tag{5.2}$$

Therefore, $X_t^{\ell=31}$ consists of 416 real-valued features used to predict r_t. Afterwards, the rolling window constructor move to $t+1$ (if available, otherwise move to the next day with valid returns) and generate another pair of feature and target (X_{t+1}, r_{t+1}).

Finally, the rolling window generates 4,934 pairs of (X_t, r_t), in which t ranges from January 1, 2000 to September 30, 2019. Among the 4,934 samples, each X_t is a 416 dimensional real-valued vector and r_t is a real-valued scalar. This paper uses samples (X_t, r_t) with t before January 1, 2019 as training set (4,747 samples) and the rest of samples are taken as test set (187 samples).

$$\mathcal{D}^{\text{train}} := \{(X_t, r_t) : t \leq \text{December 31, 2018}\} \tag{5.3}$$

$$\mathcal{D}^{\text{test}} := \{(X_t, r_t) : t \geq \text{January 1, 2019}\} \tag{5.4}$$

After assessing models' performances on the test set, $\mathcal{D}^{\text{train}}$ and $\mathcal{D}^{\text{test}}$ are further split into 5 subsets [7] to explore the effectiveness of models on each day of the week.

[7] (X_t, r_t) are split based on which day of the week t is. There are only 5 groups since r_t are always missing

5.1.3 Performance Metrics

In order to quantify the performance of a predictive model, we have to specify a performance metric measuring the proximity between predictions and actual values. Let $\hat{r}_t$ denote the predicted value of r_t, the performance metric should reflect the proximity between predicted and true returns. The primary performance metric used in this paper is the mean squared error (MSE). The MSE of a model aiming to predict $\{r_1, r_2, \cdots, r_T\}$ is defined as

$$MSE := \frac{1}{T}\sum_{t=1}^{T}(r_t - \hat{r}_t)^2 \tag{5.5}$$

One advantage of MSE metric is that it is differentiable with respect to each $\hat{r}_t$, this differentiability allows us to train models on this dataset using back-propagation algorithm (Hecht-Nielsen 1989). Even though not all predictive models in this paper are based on back-propagation or require differentiable objective functions, we use MSE to as the primary metric to select and evaluate models for consistency.

Unfortunately, the MSE is not naturally interpretable, and MSE changes when the unit of returns switches to percentage returns. We introduce anther widely used error metric, directional accuracy (DA) defined as following:

$$DA := \frac{1}{T}\sum_{t=1}^{T}\mathbb{1}\{\text{sign}(r_t) = \text{sign}(\hat{r}_t)\} \tag{5.6}$$

The directional accuracy measures the frequency that the model predict the sign of return correctly. The directional accuracy can be interpreted easily, but it is not differentiable.

5.1.4 Model Selection and Randomized Cross Validation

After choosing a class of predictive models, one still needs to select a set of hyper-parameters (i.e., model configurations), $\theta \in \Theta$. In subsequent discussions, we use subscript $\mathcal{M}_\theta$ to denote a model with configuration θ from class $\mathcal{M}$. For example, suppose $\mathcal{M}$ is the class of all polynomial regressions, then one hyper-parameter is the maximum degree in the regression equation. In this case, the set of possible hyper-parameters, Θ, is all positive

when t is weekend.

integers. One has to choose the optimal maximum degree θ^* from Θ so that $\mathcal{M}_\theta^*$ has the best (test-time) performance.

Choosing the optimal θ^* is crucial for building effective predictive algorithms, simply choosing a super complicated model would over-fit the training set and leads to poor test-time performance (Claeskens and Hjort 2008).

For each predictor class $\mathcal{M}$ and corresponding space of hyper-parameters Θ, we firstly determine the optimal hyper-parameter $\theta^* \in \Theta$ using a 5-fold randomized cross validation algorithm (5-fold RCV).

Figure 25: 5-fold Randomized Cross Validation

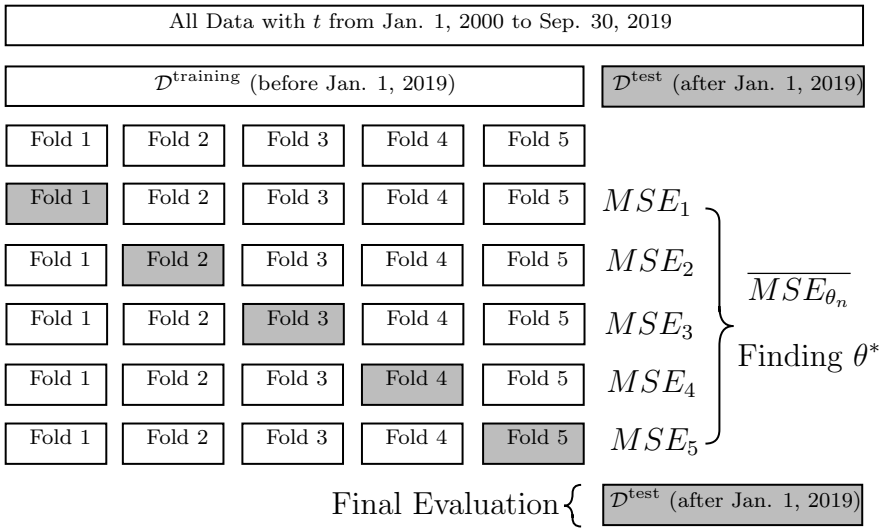

Firstly, N candidates of hyper-parameters $\{\theta_1, \theta_2, \cdots, \theta_N\}$ are sampled from a uniform distribution on Θ (i.e., the randomized part in RCV). Then, for each $\theta_n \in \{\theta_1, \theta_2, \cdots, \theta_N\}$, θ_n defines a predictive model $\mathcal{M}_{\theta_n}$ Figure 25 illustrates the cross validation procedure for one hyper-parameter set θ_n. The entire $\mathcal{D}^{\text{train}}$ are split into 5 equal consecutive subsets (called folds): $\mathcal{D}_i^{\text{train}}$ for $i \in \{1, 2, 3, 4, 5\}$. Then, $\mathcal{M}_{\theta_n}$ is fitted on $\cup_{i\in\{1,2,3,4\}}\mathcal{D}_i^{\text{train}}$ (training set) and evaluated on $\mathcal{D}_5^{\text{train}}$ (validation set), let $\widehat{MSE}_5$ denote mean squared error of this model on $\mathcal{D}_5^{\text{train}}$. Afterwards, the same model is fitted again on $\cup_{i\in\{1,2,3,5\}}\mathcal{D}_i^{\text{train}}$, evaluated on $\mathcal{D}_4^{\text{train}}$ and leads to another error metric $\widehat{MSE}_4$. The same procedure can be repeated for five times with different validation set and creates five mean squared error metrics. Let $\overline{MSE}_{\theta_n}$ denote the average of $\widehat{MSE}_1$ to $\widehat{MSE}_5$ using hyper-parameter θ_n. Then, $\overline{MSE}_{\theta_n}$ constitutes an

estimated test-time performance of model $\mathcal{M}_{\theta_n}$ on $\mathcal{D}^{\text{test}}$ when it is fitted on $\mathcal{D}^{\text{train}}$. Among the N candidates of hyper-parameters for model class $\mathcal{M}$, we choose θ_n with the smallest $\overline{MSE}_{\theta_n}$ to be the best-performing parameter, denoted as θ^*. This θ^* is not necessarily the truly best one among all θ in Θ, θ^* is only the best-performing configuration within N samples. However, since we sampled the N candidates uniformly from Θ, performance of the selected θ^* should be close to the truly optimal configuration especially when N is sufficiently large.

While using 5-fold RCV and N sampled θ, we need for fit $5N$ models from class $\mathcal{M}$ in total to determine the optimal configuration θ^* for this model class. Clearly, the larger N is the more likely for us to include the truly optimal configuration in our sampled configurations. Specifically, we choose N to be 500 in this paper.

Since this paper works with two performance metrics: mean-squared-error (MSE) and directional accuracy (DA), there are at least two criterions to identify the optimal model.

MSE-Optimal The first selection criterion identifies the optimal model from a given model class based on models' validation MSEs. Given a class of models, one model is the MSE-optimal of this model class if

- this model achieves at least a DA of 50% on the validation set;
- and, it achieves the lowest MSE on the validation set among all models satisfy the first condition.

If there are more than one models with the same lowest validation MSE and DA greater than 50%, we will choose the one with the best DA to be the optimal model. This type of model identifying method based on validation MSE is called **randomized cross validation with mean squared error** (RCV-MSE) in this paper.

DA-Optimal The second criterion selects the best model from candidates based on their validation DAs. Given a class of models, one model is the DA-optimal of this model class if

- this model achieves the highest DA on the validation set.

If there are multiple models with the same lowest accuracy, the model with the lowest validation MSE is chosen to be the DA-optimal. This kind of searching technology that identifies the optimal model based on validation DA is referred to as **randomized cross validation with directional accuracy** (RCV-DA).

Let $\mathcal{M}^{\text{MSE}}_{\text{model class}}$ and $\mathcal{M}^{\text{DA}}_{\text{model class}}$ denote the MSE-optimal and DA-optimal models from a particular model class. After identifying optimal models, the performances of $\mathcal{M}^{\text{MSE}}_{\text{model class}}$ and $\mathcal{M}^{\text{DA}}_{\text{model class}}$ on the test set will be proxies of the performance of the specified model class on the prediction task. Note that these optimal models can be identify completely without the test set, therefore, evaluating them on the test set mimics real-world environment: someone builds and trains a model at time t using all information available up to time t, then the model is implemented on company's server and used in production after day t. What traders really care about is the predictive model's performance after day t, called test time performance, since the test time performance is directly related to the profitability of any trading algorithms built on this predictive model. Therefore, one model's performance on the test set is a fair proxy for the business value of this model in real-world.

5.2 Baseline Models: The Naive Predictor and Moving Average Predictors

To answer the first research question, whether crude oil returns are predictable, we need to firstly define several dummy models for benchmarking purpose. Recall that this paper defines two separate information sets:

- Ω_{partial} denotes the information set containing historical returns only.
- Ω_{complete} denotes the information set consisting of both historical returns and news sentiments.

Predictive models based on Ω_{partial} only use 31 lagged returns to predict future returns, in contrast, models based on Ω_{partial} utilizes all 416 features including lagged returns and features extracted from news sentiments.

If a model $\mathcal{M}$ based on $\Omega \in \{\Omega_{\text{partial}}, \Omega_{\text{partial}}\}$ fails to out-perform baseline models on the test set, then we may conclude the crude oil market is efficient (i.e., unpredictable) with respect to this model and information set Ω.

The simplest model is a **naive predictor**, $\mathcal{M}_{\text{naive}}$, based on the martingale assumption on crude oil prices. This model assumes the close spot price p_t on day t to be exactly the close price on the previous day. Therefore, $\mathcal{M}_{\text{naive}}$ is predicting zero returns all the time.

$$\hat{r}_t = \mathcal{M}_{\text{naive}} = 0 \tag{5.7}$$

In addition, we define other **moving-average predictors** [8] denoted as $\mathcal{M}_{\text{MA}(k)}$, where k is a positive integer representing the scope of this model. To predict return r_t, the model $\mathcal{M}_{\text{MA}(k)}$ looks into the past k trading days and predicts the return to be the average return of them.

$$\hat{r}_t = \mathcal{M}_{\text{MA}(k)} = \frac{1}{k} \sum_{\tau=t-k}^{t-1} r_\tau \tag{5.8}$$

As mentioned before, this paper uses all data before December 31, 2018 as the training set (4,746 trading days) and data from January 1, 2019 to October 31, 2019 as the test set (187 trading days). Table 14 presents performances of benchmark models in terms of mean-squared-error (MSE) and directional accuracy (DA).

Table 14: Performances of Benchmark Models

Model	Training MSE	Training DA	Testing MSE	Testing DA
$\mathcal{M}_{\text{naive}}$	4.655	0.716%	4.057	0.538%
$\mathcal{M}_{\text{MA(5)}}$	5.612	50.274%	4.693	50.000%
$\mathcal{M}_{\text{MA(25)}}$	4.811	50.295%	4.248	50.000%
$\mathcal{M}_{\text{MA(50)}}$	4.725	49.536%	4.261	50.000%
$\mathcal{M}_{\text{MA(100)}}$	4.706	49.241%	4.226	44.624%
$\mathcal{M}_{\text{MA(300)}}$	4.676	47.977%	4.060	48.925%

Note that the directional accuracy of $\mathcal{M}_{\text{naive}}$ model is nearly zero on both training and testing sets because returns are rarely exactly zero in the dataset. As we expected, those

[8] The moving-average predictors is not related to ARIMA models introduced later.

benchmark models are too simple to achieve better performances than random guessing (i.e., 50% directional accuracy). This preliminary analysis on benchmark models' performances leads to Conclusion 5.1.

Conclusion 5.1. These results suggest that the crude oil market is efficient (i.e., unpredictable) with respect to

(i) the information set Ω_{partial} containing historical returns

(ii) and both native predictor and moving-average predictors.

Then we are going to examine whether other more sophisticated models based on Ω_{partial} can attain significantly better test time performances than those above-mentioned benchmark models.

After evaluating performances of these benchmark models, we can answer the two research questions using the following Rule 5.1 and Rule 5.2.

Rule 5.1 (Research Question 1)**.** Given an information set $\Omega \in \{\Omega_{\text{partial}}, \Omega_{\text{complete}}\}$, a class of models and a model searching technology, let $\mathcal{M}^*$ denote the optimal model identified. Then the crude oil market is claimed to be predictable (i.e., inefficient) if (i) the testing MSE of $\mathcal{M}^*$ is lower than MSE values of benchmark models and (ii) the testing DA of $\mathcal{M}^*$ is higher than 50%.

Rule 5.2 (Research Question 2)**.** Given a class of models and searching technology, let $\mathcal{M}^*_{\Omega_{\text{partial}}}$ and $\mathcal{M}^*_{\Omega_{\text{complete}}}$ denote optimal models on two information sets identified by the searching technology. Then this paper concludes that we can better predict returns by incorporating news sentiments if (i) $\mathcal{M}^*_{\Omega_{\text{complete}}}$ has better testing MSE and testing DA than $\mathcal{M}^*_{\Omega_{\text{partial}}}$ and (ii) testing MSE of $\mathcal{M}^*_{\Omega_{\text{complete}}}$ is lower than benchmark MSEs and testing DA of $\mathcal{M}^*_{\Omega_{\text{complete}}}$ is higher than 50%.

In order to claim news sentiment are helpful, Rule 5.2 requires $\mathcal{M}^*_{\Omega_{\text{complete}}}$ to be an useful model.

5.3 Linear Models: Autoregressive Integrated Moving Average

One classical model used for time series forecasting is the autoregressive integrated moving average (ARIMA) model.

The autoregressive moving average (ARMA) models the return at time step t, r_t, as a function the series itself and a series of error terms. In particular, an ARMA(p, q) process identifies r_t as a linear combination of p lagged variation of r_t and q noise terms:

$$X_t - \phi_1 X_{t-1} - \cdots - \phi_p X_{t-p} = \varepsilon_t + \theta_1 \varepsilon_{t-1} + \cdots + \theta_q \varepsilon_{t-q} \tag{5.9}$$

More concisely, let L denote the lag operator, an ARMA(p,q) process can be written with the more compact notion

$$\Phi_p(L) r_t = \Theta_q(L) \varepsilon_t \tag{5.10}$$

where $\Phi_p(\cdot)$ and $\Theta_q(\cdot)$ are polynomials up to degree p and q respectively.

One crucial assumption on $\{r_t\}$ is that it has to be stationary. To handle non-stationary processes, one can apply the differencing operator, $1 - L$, iteratively until the differenced series becomes stationary. If the stationarity is achieved after d iterations of differencing, the original series is said to be integrated of order d and can be modelled using an ARIMA(p, d, q) model:

$$\Phi_p(L)(1 - L)^d X_t = \Theta_q(L) \varepsilon_t \tag{5.11}$$

ARIMA models the inter-temporal dependencies naturally, however, ARIMA can only handle linear relationships. In later sections, non-linear models such as support vector machines will be introduced.

Since ARIMA models work on univariate time series only, we are only assessing whether the market is efficient with respect to ARIMA models and the partial information set Ω_{partial}.

Instead of cross validation, the optimal model is identified based on Akaike's information criterion (AIC). For a given ARIMA model, let k denote the number of parameters in this model, the value of k is positively correlated with the model's complexity. Let L denote the maximum value of likelihood function of this model on the training set. The AIC of this

model is defined in equation (5.12).

$$AIC = 2k - \ln(L) \tag{5.12}$$

Since simpler models are less likely to overfit the training set and can generalize better. The AIC penalizes model complexity and rewards log-likelihood, therefore, minimizing AIC seeks for a balance between the model's complexity and training set performance.

One ARIMA model can be uniquely specified by a set of orders (p, d, q). This paper trains all ARIMA models with $6 \times 3 \times 6 = 72$ different combinations of (p, d, q) specified in Table 15. The model attains the lowest AIC is identified to be the optimal model. For generality, this paper reports the best three models. It turns out that ARIMA(5,0,5), ARIMA(4,0,3) and ARIMA(5,0,4) are the three models attain the lowest three AIC values on training set. Table 16 summarizes the performances of these three optimal models identified.

Table 15: Scope of Orders for ARIMA

Parameter	Scope
p	{0,1,2,3,4,5}
d	{0,1,2}
q	{0,1,2,3,4,5}

Table 16: Performances of Linear Models

Model	Testing MSE	Testing DA
$\mathcal{M}_{\text{ARIMA(5,0,5)}}$	4.074	50.763 %
$\mathcal{M}_{\text{ARIMA(4,0,3)}}$	4.070	51.156 %
$\mathcal{M}_{\text{ARIMA(5,0,4)}}$	4.073	50.567 %

Performances of these models suggest that ARIMA models can hardly achieve a better-than-guessing accuracy. Moreover, in terms of test time MSE, all three ARIMA models preform poorly compared with naive predictor, which achieves testing MSE of 4.057. Such unsatisfactory performances suggest the crude oil return is essentially unpredictable using ARIMA models based on the partial information set. Therefore, we can extend our previous finding to Conclusion 5.2.

Conclusion 5.2. The crude oil market is efficient with respect to

(i) Information set: the information set Ω_{partial} containing historical returns.

(ii) Model Class: ARIMA models.

(iii) Searching Technology: the model attaining the lowest AIC on training set is identified to be the optimal model.

5.4 Support Vector Regression

The previous section shows that the crude oil market is efficient with respect to linear models. In contrast, this section is devoted to non-linear models and answers whether the market is efficient against non-linear models.

Support vector machines (SVM) was firstly proposed by Boser, Guyon and Vapnik as a classification method for hand-written digit recognition (1992). Over the past three decades, SVM has been believed to be the best off-the-shelf classification algorithm.

As mentioned in section 5.1.1, characteristic functions generate 416 predictors in total for each one target r_t, so that the prediction task is in fact a high dimensional problem. SVM models only focus a few training samples termed *support vectors*, therefore, SVMs often produce promising results on high dimensional problems.

Moreover, by using different *kernel functions*, SVMs are capable of transforming these raw features to an even higher dimensional space. For example, if one wishes to classify points in $\mathbb{R}^2$, other algorithms like logistic regressions would classify the point based on $(x_1, x_)$ directly and maps (x_1, x_2) to class labels. Instead, a SVM with polynomial kernel of degree two will classify the point based all combinations of (x_1, x_2) up to degree two, that is, $(x_1, x_2, x_1^2, x_1x_2, x_2^2) \in \mathbb{R}^5$. In this case, the original 2-dimensional input space is transformed into a 5-dimensional feature space by the kernel function. While a SVM is using the Radial Basis Function (RBF) kernel, the original input space is transformed into an infinite-dimensional feature space. This implicit feature engineering enables SVM to explore more complex patterns in the dataset. Smola and Scholkorf provide a detailed review of training SVMs and theories behind kernel functions in their work (2004).

A few years after the SVM was proposed as a classifier, Drucker and others proposed an extension to original SVM called support vector regression machines (SVR) (Drucker et al. 1997). As the name suggests, SVR is designed for regression problems. It has been shown that SVRs perform reasonably well on high dimensional regression problems by focusing on a few support vectors and engineering features implicitly using kernel functions.

As mentioned in Smola and Scholkorf's work, performances of support vector machines are determined by several hyper-parameters listed in Table 17. To choose the optimal configuration of SVR in this paper's prediction task, a RCV algorithm samples 500 configurations from the scope of hyper-parameters in Table 17 and evaluates each configuration based on their MSE and DA on the validation set.

Table 17: Scope of Hyper-parameters for Support Vector Regression Machines

Hyper-parameter	Scope
Kernel Type	{Radial Basis Function (RBF) kernel}
γ	$\{10^{-10}, 10^{-9}, 10^{-8}, 10^{-7}, 10^{-6}, 10^{-5}, 10^{-4}, 10^{-3}, 10^{-2}, 0.1, 1, 10\}$
Tolerance	$\{10^{-10}, 10^{-9}, 10^{-8}, 10^{-7}, 10^{-6}, 10^{-5}, 10^{-4}, 10^{-3}, 10^{-2}, 0.1, 1, 10\}$
ε	$\{10^{-10}, 10^{-9}, 10^{-8}, 10^{-7}, 10^{-6}, 10^{-5}, 10^{-4}, 10^{-3}, 10^{-2}, 0.1, 1, 10\}$
C	$\{10^{-10}, 10^{-9}, 10^{-8}, 10^{-7}, 10^{-6}, 10^{-5}, 10^{-4}, 10^{-3}, 10^{-2}, 0.1, 1, 10\}$

Table 18 and Table 19 presents the optimal models under both criterions and their respective performances.

Table 18: Optimal Hyper-parameters for Support Vector Regression Machines

Model	Kernel	γ	Tolerance	ε	C
For Ω_{partial}					
$\mathcal{M}_{\text{SVR}}^{\text{MSE}}$	RBF	0.1	10^{-2}	1	1
$\mathcal{M}_{\text{SVR}}^{\text{DA}}$	RBF	0.1	10^{-7}	10^{-6}	1
For Ω_{complete}					
$\mathcal{M}_{\text{SVR}}^{\text{MSE}}$	RBF	10^{-6}	1	10^{-3}	10^{-9}
$\mathcal{M}_{\text{SVR}}^{\text{DA}}$	RBF	10^{-7}	10^{-5}	10^{-7}	10

Table 19: Performances of Support Vector Regression Machines

Model	Validation MSE	Validation DA	Testing MSE	Testing DA
Trained on Ω_{partial}				
$\mathcal{M}_{\text{SVR}}^{\text{MSE}}$	4.654	51.033%	4.036	52.941%
$\mathcal{M}_{\text{SVR}}^{\text{DA}}$	4.655	51.833%	4.040	53.476%
Trained on Ω_{complete}				
$\mathcal{M}_{\text{SVR}}^{\text{MSE}}$	4.655	51.433%	4.055	54.301%
$\mathcal{M}_{\text{SVR}}^{\text{DA}}$	4.830	51.665%	4.399	49.462%

The MSE-optimal SVR, $\mathcal{M}_{\text{SVR}}^{\text{MSE}}$, out-performs benchmark models and ARIMA models examined before. Using either Ω_{parital} or Ω_{complete}, $\mathcal{M}_{\text{SVR}}^{\text{MSE}}$ achieves better test time DA compared with the random-guessing-accuracy. Hence, this paper concludes the market is essentially predictable with respect to both information sets and SVR-optimal support vector regression machines. In contrast, test time performances of the DA-optimal SVR trained on Ω_{complete} suggest that the market is efficient in this case. Conclusion 5.3 summarizes answers to the first research question.

Conclusion 5.3.

Model Class	Information Set	Searching Technology	Efficient or Not
SVR	Ω_{parital}	RCV-MSE	Inefficient
SVR	Ω_{parital}	RCV-DA	Inefficient
SVR	Ω_{complete}	RCV-MSE	Inefficient
SVR	Ω_{complete}	RCV-DA	Efficient

As for the second research question, even though both $\mathcal{M}_{\text{SVR}}^{\text{MSE}}$ on Ω_{partial} and on Ω_{complete} attain lower test time MSE than benchmark models and ARIMA models, there is no improvement by utilizing the complete information set (4.055 MSE) instead of the partial information set (4.036 MSE). Moreover, the DA-optimal SVR trained on Ω_{complete} performs even worse than the DA-optimal SVR trained on Ω_{partial}. Above observations lead to Conclusion 5.4 and Conclusion **??**, which answer the second research question.

Conclusion 5.4. While using support vector machines as predictive models and RCV-MSE searching technology, incorporating news sentiment dataset does not help predict crude oil returns.

Conclusion 5.5. While using RCV-DA searching technology, adding news sentiment features even hurt the performance of support vector machines.

Lastly, the two conclusions above suggest that if one wishes to extend current SVR-based predictive models to incorporate news sentiment features, RCV-MSE is a dominant strategy to identify the optimal model.

5.5 Random Forests

Another class of non-linear methods used widely is the random forest. Breiman proposed an ensemble model based on traditional tree methods called random forest (2001). A forest as an ensemble of independently trained trees reduces the variance of prediction and achieves a better performance compared with one single tree predictor. Let p denote the number of independent variables for prediction ($p = 416$ here). Training each tree in the forest using all p features can cause over-fitting problems and lead to poor test time performance. Therefore, each independent tree predictor in the forest is trained only using a random subset of p features, which constitutes the randomness of a random forest. This randomness on feature selection helps random forests to generalize better and achieves even lower loss on the test set. Typically, each tree in the forest is only trained on $\log_2(p)$ features.

Table 20 enumerates key hyper-parameters of a random forest predictor and corresponding scopes our cross validation procedure searches over.

Table 20: Scope of Hyper-parameters for Random Forests

Hyper-parameter	Scope
n Number of trees	$\{1, 2, 3, \cdots, 200\}$
f Max num. of features for each tree	$\{p, \log_2(p)\}$
d Max depth of each tree	$\{10, 14, 19, 24, \cdots, 100, 105, 110, \infty\}$
m_1 Min amount of samples required to split an internal node	$\{2, 5, 10\}$
m_2 Minimum number of samples required at each leaf node	$\{1, 2, 4\}$
What dataset is used to construct each tree	{bootstrapped samples, entire training dataset}

Table 20 summarizes configurations of $\mathcal{M}_{\text{RF}}^{\text{MSE}}$ and $\mathcal{M}_{\text{RF}}^{\text{DA}}$ identified.

Table 21: Optimal Hyper-parameters for Random Forests

Model	n	f	d	m_1	m_2	Training Samples
For Ω_{partial}						
$\mathcal{M}_{\text{RF}}^{\text{MSE}}$	41	$\log_2(p)$	10	5	1	Bootstrapped Samples
$\mathcal{M}_{\text{RF}}^{\text{DA}}$	130	p	10	10	1	Entire Training Set
For Ω_{complete}						
$\mathcal{M}_{\text{RF}}^{\text{MSE}}$	96	$\log_2(p)$	10	10	2	Bootstrapped Samples
$\mathcal{M}_{\text{RF}}^{\text{DA}}$	41	p	14	5	4	Entire Training Set

After identifying optimal models, these models are evaluated using the test set and Table 21 reports performances of random forests.

Surprisingly, random forests trained on Ω_{partial} consistently perform better than those trained on Ω_{complete} regardless of the searching technology used. Test time accuracies of models on Ω_{partial} suggest the market is predictable in this setting. Moreover, note that models on Ω_{partial} attain lower testing MSE compared with benchmark models (4.057 MSE), this observation further confirm our previous conclusion that the market is inefficient.

In contrast, random forests defined on Ω_{complete} only achieve an unsatisfactory result in terms of testing MSE. Both optimal models perform worse than a naive predictor, which attains a testing MSE of 4.057.

Table 22: Performances of Random Forests

Model	Validation MSE	Validation DA	Testing MSE	Testing DA
Trained on Ω_{partial}				
$\mathcal{M}_{\text{RF}}^{\text{MSE}}$	4.717	50.716%	4.024	53.476%
$\mathcal{M}_{\text{RF}}^{\text{DA}}$	5.325	51.243%	4.053	53.476%
Trained on Ω_{complete}				
$\mathcal{M}_{\text{RF}}^{\text{MSE}}$	4.675	50.464%	4.148	48.387%
$\mathcal{M}_{\text{RF}}^{\text{DA}}$	5.716	51.960%	4.753	53.226%

In terms of the directional accuracy, $\mathcal{M}_{\text{RF}}^{\text{DA}}$ achieves better results than random guessing on both validation and test sets. However, a market is predictable only if a model can consistently achieve better-than-guessing results. The statistics in Table 22 are not sufficient to conclude the market is predictable. It is possible that too many sentiment features are

generated in the previous section and most of them are essentially noises. Consequently, the informative content in Ω_{partial} are masked by these additional noisy signals in Ω_{complete} and random forests fail to perform well on Ω_{complete}. Findings on random forests answering the first research question are summarized in Conclusion 5.6.

Conclusion 5.6.

Model Class	Information Set	Searching Technology	Efficient or Not
RF	Ω_{parital}	RCV-MSE	Inefficient
RF	Ω_{parital}	RCV-DA	Inefficient
RF	Ω_{complete}	RCV-MSE	Efficient
RF	Ω_{complete}	RCV-DA	Efficient

The answer to the second research question is straightforward in the random forest's case.

Conclusion 5.7. It is unlikely to improve random forest's performance on crude oil return forecasting by utilizing additional news sentiment features.

5.6 Long Short-Term Memory Recurrent Neural Networks

An ARIMA model captures the intertemporal correlation among independent variables explicitly. However, ARIMA models are not capable of modelling complex non-linearities. The superior performance of SVRs indicates that considering non-linear interactions among independent variables can improve model performance significantly.

Unfortunately, even though SVRs and random forests are capable to model complex, they squeeze all independent variables and disregard the orders among independent variables. Hence, SVRs and random forests are not able to utilize information from the sequential structures (orders) of independent variables.

In current literature, neural networks have been used widely to capture non-linearity among independent variables. One special type of neural works termed recurrent neural networks (RNN) is designed to model both non-linearities and inter-temporal correlations. However, conventional RNNs suffer from vanishing and exploding gradient problems and becomes impotent on longer time series. In section 3.2, the ACF and PACF plots have

identified possible seasonality in crude oil returns. Modelling seasonality requires the RNN to pay attention to inter-temporal dependencies over a longer period of time.

Hochreiter and Schmidhuber proposed the long short-term memory (LSTM) cell for RNNs, this novel architecture allows RNNs to focus on inter-temporal dependencies over both short and long periods (1997). All RNNs trained and evaluated in this paper are based on this LSTM architecture.

Table 23 summarizes the scope of hyper-parameters for LSTM RNNs.

Table 23: Scope of Hyper-parameters for LSTM RNNS

Hyper-parameter	Scope
Epochs of training	$\{5, 6, 7, 8, \cdots, 18, 19, 20, 25, 30, 35, \cdots, 200\}$
h Size of RNN hidden layer	$\{32, 64, 128, 256, 512, 1024\}$
ℓ Number of RNN hidden layers	$\{1, 2, 3\}$
p_{rnn} Dropout probability in RNN hidden layers	$\{0, 0.25, 0.5\}$
p_{fc} Dropout probability in the output layer	$\{0, 0.25, 0.5\}$
B Batch size	$\{32, 128, 512\}$
α Learning rate	$\{10^{-5}, 3\times10^{-5}, 10^{-4}, 3\times10^{-4}, 10^{-3}, 3\times10^{-3}, 0.01, 0.03, 0.1, 0.3\}$

Table 24 and Table 25 present two optimal models and their test time performances. Because LSTM RNNs are capable to capture all of non-linearities, inter-temporal dependencies over short time periods (inter-day transitions) and inter-temporal dependencies over longer time periods (seasonalities), both $\mathcal{M}^{\text{MSE}}_{\text{LSTM}}$ and $\mathcal{M}^{\text{DA}}_{\text{LSTM}}$ out-perform all other models implemented earlier in this paper.

Table 24: Optimal Hyper-parameters for LSTM RNNs

Model	Epochs	h	ℓ	p_{rnn}	p_{fc}	B	α
For Ω_{partial}							
$\mathcal{M}^{\text{MSE}}_{\text{LSTM}}$	8	512	3	0.5	0.5	32	3×10^{-4}
$\mathcal{M}^{\text{DA}}_{\text{LSTM}}$	155	32	3	0.5	0.0	512	0.1
For Ω_{complete}							
$\mathcal{M}^{\text{MSE}}_{\text{LSTM}}$	40	32	2	0.0	0.5	512	10^{-5}
$\mathcal{M}^{\text{DA}}_{\text{LSTM}}$	12	128	2	0.0	0.25	512	10^{-5}

Table 25: Performances of LSTM RNNs

Model	Validation MSE	Validation DA	Testing MSE	Testing DA
Trained on Ω_{partial}				
$\mathcal{M}_{\text{LSTM}}^{\text{MSE}}$	3.992	52.450%	4.044	44.385%
$\mathcal{M}_{\text{LSTM}}^{\text{DA}}$	4.668	53.792%	4.045	54.011%
Trained on Ω_{complete}				
$\mathcal{M}_{\text{LSTM}}^{\text{MSE}}$	4.192	51.609%	4.043	54.012%
$\mathcal{M}_{\text{LSTM}}^{\text{DA}}$	4.888	54.480%	4.041	54.011%

Statistics in Table 25 suggest that testing MSE values of LSTM-RNN are always below MSE values of benchmark models. Even though $\mathcal{M}_{\text{LSTM}}^{\text{MSE}}$ on Ω_{partial} does not perform well in terms of testing DA (44.385%), its performance is improved significantly to 54.012% after switching to Ω_{complete}. This observation serves as an evidence implying that including news sentiment can help crude oil forecasting. Overall, Conclusion 5.8 and Conclusion 5.9 answer the first and the second research question of this thesis.

Conclusion 5.8. The efficiencies of crude oil market with respect to LSTM-RNN, various information sets and searching technologies are summarized as:

Model Class	Information Set	Searching Technology	Efficient or Not
LSTM-RNN	Ω_{parital}	RCV-MSE	Efficient
LSTM-RNN	Ω_{parital}	RCV-DA	Inefficient
LSTM-RNN	Ω_{complete}	RCV-MSE	Inefficient
LSTM-RNN	Ω_{complete}	RCV-DA	Inefficient

Conclusion 5.9. A LSTM-RNN selected using RCV-MSE can leverage the predictive power of news sentiment. That is, and crude oil market can be better predicted by including news sentiments.

5.7 Taking the Day-of-the-Week Effect into Consideration

In section 3.3, we have shown that crude oil returns experience the day-of-the-week effect. In particular, the empirical distribution of Mondays' returns is significantly different from distributions of other days. Moreover, Mondays are more likely to experience negative returns

compared with other days. Therefore, it is reasonable to conjecture that the underlying dynamics of returns on Mondays might be different from the dynamics of returns of other days. Recall that the original dataset built upon Ω_{complete} consists of 4,933 pairs of (X_t, r_t) and each feature vector $X_t \in \mathbb{R}^{416}$. Among the 4,932 feature-target pairs (X_t, r_t), targets of the first 4,746 pairs are returns before December 31, 2018 and these pairs are used as the training set. In contrast, the last 186 pairs serve as the testing set.

To examine the potential benefits from building different models for different days of the week, training and testing sets are split into two training and two testing sets.

- Training set (Monday) consists of samples (X_t, r_t) from the original training set such that t is a Monday (889 samples).
- Testing set (Monday) consists of samples (X_t, r_t) from the original testing set such that t is a Monday (34 samples).
- Training set (other days) consists of samples (X_t, r_t) from the original training set such that t is not a Monday (3,857 samples).
- Testing set (other days) consists of samples (X_t, r_t) from the original testing set such that t is a not Monday (152 samples).

The same RCV-MSE and RCV-DA techniques are applied on the two training sets to identify the corresponding MSE-optimal and DA-optimal models for returns on Mondays and other days. Table 26, Table 27 and Table 28 report optimal models for each dataset. Notations for optimal models are similar as before, for example, $\mathcal{M}^{\text{MSE}}_{\text{RF, Mondays}}$ represents the MSE-optimal random forest for predicting returns on Mondays and $\mathcal{M}^{\text{MSE}}_{\text{SVR, Other Days}}$ indicates the MSE-optimal SVR for predicting returns on Tuesdays, Wednesdays, Thursdays and Fridays.

Table 26: Optimal Hyper-parameters for Random Forests on Restricted Datasets

Model	n	f	d	m_1	m_2	Training Samples
$\mathcal{M}^{\text{MSE}}_{\text{RF, Mondays}}$	115	$\log_2(p)$	38	10	4	Bootstrapped Samples
$\mathcal{M}^{\text{DA}}_{\text{RF, Mondays}}$	116	$\log_2(p)$	38	2	1	Entire Training Set
$\mathcal{M}^{\text{MSE}}_{\text{RF, Other Days}}$	88	$\log_2(p)$	10	5	4	Bootstrapped Samples
$\mathcal{M}^{\text{DA}}_{\text{RF, Other Days}}$	157	p	10	2	1	Entire Training Set

Table 27: Optimal Hyper-parameters for Support Vector Regressions on Restricted Datasets

Model	Kernel	γ	Tolerance	ε	C
$\mathcal{M}^{\text{MSE}}_{\text{SVR, Mondays}}$	RBF	10^{-10}	10^{-3}	10^{-4}	10
$\mathcal{M}^{\text{DA}}_{\text{SVR, Mondays}}$	RBF	10^{-6}	0.1	10^{-6}	1
$\mathcal{M}^{\text{MSE}}_{\text{SVR, Other Days}}$	RBF	0.1	0.1	10^{-4}	10
$\mathcal{M}^{\text{DA}}_{\text{SVR, Other Days}}$	RBF	10^{-9}	0.1	10^{-7}	1

Table 28: Optimal Hyper-parameters for LSTM RNNs on Restricted Dataset

Model	Epochs	h	ℓ	p_{rnn}	p_{fc}	B	α
$\mathcal{M}^{\text{MSE}}_{\text{LSTM, Mondays}}$	45	128	2	0.5	0.0	128	10^{-4}
$\mathcal{M}^{\text{DA}}_{\text{LSTM, Mondays}}$	75	1024	3	0.0	0.25	128	0.01
$\mathcal{M}^{\text{MSE}}_{\text{LSTM, Other Days}}$	14	512	3	0.0	0.5	32	0.001
$\mathcal{M}^{\text{DA}}_{\text{LSTM, Other Days}}$	12	512	3	0.0	0.0	32	0.001

After optimal models for each dataset are identified, the are evaluated on the corresponding testing sets. Performances of models are reported in Table 29, best performances are in bold font. As we have expected, optimal models for both datasets are from LSTM RNN class since LSTM-RNNs are capable of capturing both key factors in time series forecasting task: non-linearities and inter-temporal correlations. In particular, $\mathcal{M}^{\text{MSE}}_{\text{LSTM, Mondays}}$ achieves a superior performance in terms of the directional accuracy in the test set.

The test-time performance of using two separate models can be estimated by taking the weighted average of loss/accuracy on two testing sets using equation (5.13). Let $\mathcal{M}_A$ and $\mathcal{M}_B$ denote models used for Mondays and other days in the joint model. The joint model uses $\mathcal{M}_A$ to make prediction every Monday and uses $\mathcal{M}_B$ on other days.

$$\begin{aligned}\text{Performance} \approx{}& \%\text{ of Mondays} \times \mathcal{M}_A\text{'s test performance} + \%\text{ of other days} \times \mathcal{M}_B\text{'s test performance} \\ ={}& \frac{34}{186} \times \mathcal{M}_A\text{'s test time performance} + \frac{152}{186} \times \mathcal{M}_B\text{'s test time performance}\end{aligned} \tag{5.13}$$

all three types of models used are data-intensive but there are only 889 training samples of Mondays. Therefore, none of them delivers a significantly better result compared with

models previously trained using the entire dataset.

Table 29: Performances of Models on Restricted Datasets

Model	Validation MSE	Validation DA	Testing MSE	Testing DA
$\mathcal{M}^{\text{MSE}}_{\text{SVR, Mondays}}$	0.659	52.984%	0.943	41.176%
$\mathcal{M}^{\text{DA}}_{\text{SVR, Mondays}}$	0.681	54.887%	1.042	44.118%
$\mathcal{M}^{\text{MSE}}_{\text{RF, Mondays}}$	0.655	55.574%	0.919	47.059%
$\mathcal{M}^{\text{DA}}_{\text{RF, Mondays}}$	0.672	56.461%	**0.939**	55.882%
$\mathcal{M}^{\text{MSE}}_{\text{LSTM, Mondays}}$	**0.484**	51.479%	0.971	**57.143**%
$\mathcal{M}^{\text{DA}}_{\text{LSTM, Mondays}}$	0.673	**56.819**%	1.080	42.857%
$\mathcal{M}^{\text{MSE}}_{\text{SVR, Other Days}}$	5.575	52.605%	4.762	53.289%
$\mathcal{M}^{\text{DA}}_{\text{SVR, Other Days}}$	5.583	52.631%	4.776	53.289%
$\mathcal{M}^{\text{MSE}}_{\text{RF, Other Days}}$	5.606	50.997%	4.799	46.711%
$\mathcal{M}^{\text{DA}}_{\text{RF, Other Days}}$	6.844	52.449%	5.499	51.974%
$\mathcal{M}^{\text{MSE}}_{\text{LSTM, Other Days}}$	**4.947**	51.255%	**4.749**	**53.290**%
$\mathcal{M}^{\text{DA}}_{\text{LSTM, Other Days}}$	5.761	**54.836**%	4.760	**53.290**%

6 Conclusions

References

BAKER, MALCOLM, and JEFFREY WURGLER. 2006. "Investor Sentiment and the Cross-Section of Stock Returns". *The Journal of Finance* 61 (4): 1645–1680. ISSN: 0022-1082. doi:10.1111/j.1540-6261.2006.00885.x.

Baumeister, Christiane, and Lutz Kilian. 2016. "Forty Years of Oil Price Fluctuations: Why the Price of Oil May Still Surprise Us". *Journal of Economic Perspectives* 30 (1): 139–160. ISSN: 0895-3309. doi:10.1257/jep.30.1.139.

Bodnaruk, Andriy, Tim Loughran, and Bill McDonald. 2015. "Using 10-K Text to Gauge Financial Constraints". *Journal of Financial and Quantitative Analysis*.

Boser, Bernhard E, Isabelle M Guyon, and Vladimir N Vapnik. 1992. "A training algorithm for optimal margin classifiers". *Proceedings of the fifth annual workshop on Computational learning theory*: 144–152. doi:10.1145/130385.130401.

Brandt, Michael W, and Lin Gao. 2019. "Macro fundamentals or geopolitical events? A textual analysis of news events for crude oil". *Journal of Empirical Finance* 51 (J. Finance 59 3 2004): 64–94. ISSN: 0927-5398. doi:10.1016/j.jempfin.2019.01.007.

Breiman, Leo. 2001. "Random Forests". *Machine Learning* 45 (1): 5–32. ISSN: 0885-6125. doi:10.1023/a:1010933404324.

Bybee, Leland, et al. 2019. "The Structure of Economic News". *SSRN Electronic Journal*. doi:10.2139/ssrn.3446225.

Claeskens, Gerda, and Nils Lid Hjort. 2008. *Model Selection and Model Averaging*. Cambridge Books. Cambridge University Press. ISBN: 9780521852258. https://ideas.repec.org/b/cup/cbooks/9780521852258.html.

Deeney, Peter, et al. 2015. "Sentiment in oil markets". *International Review of Financial Analysis* 39:179–185. ISSN: 1057-5219. doi:10.1016/j.irfa.2015.01.005.

Drucker et al. 1997. "Support vector regression machines". *Advances in neural information processing systems*: 155–161.

Fama, Eugene F. 1970. "Efficient Capital Markets: A Review of Theory and Empirical Work". *The Journal of Finance* 25:383–417.

– . 1991. "Efficient Capital Markets: II". *The Journal of Finance* 46 (5): 1575–1617. ISSN: 0022-1082. doi:10.1111/j.1540-6261.1991.tb04636.x.

Friedman, Jerome H. 1997. "On Bias, Variance, 0/1—Loss, and the Curse-of-Dimensionality". *Data Mining and Knowledge Discovery* 1 (1): 55–77. ISSN: 1384-5810. doi:10.1023/a:1009778005914.

Gibbons, Michael R, and Patrick Hess. 1981. "Day of the Week Effects and Asset Returns". *The Journal of Business* 54 (4): 579. ISSN: 0021-9398. doi:10.1086/296147.

Hecht-Nielsen. 1989. "Theory of the backpropagation neural network". *International 1989 Joint Conference on Neural Networks*: 593–605 vol.1. doi:10.1109/ijcnn.1989.118638.

Hochreiter, Sepp, and Jürgen Schmidhuber. 1997. "Long Short-Term Memory". *Neural Computation* 9 (8): 1735–1780. ISSN: 0899-7667. doi:10.1162/neco.1997.9.8.1735.

Hodges, J L. 1958. "The significance probability of the smirnov two-sample test". *Arkiv för Matematik* 3 (5): 469–486. ISSN: 0004-2080. doi:10.1007/bf02589501.

Hu, Ziniu, et al. 2018. "Listening to Chaotic Whispers": 261–269. doi:10.1145/3159652.3159690. eprint: 1712.02136.

Jensen, Michael C. 1978. "Some anomalous evidence regarding market efficiency". *Journal of Financial Economics* 6 (2-3): 95–101. ISSN: 0304-405X. doi:10.1016/0304-405x(78)90025-9.

Loughran, Tim, and Bill McDonald. 2016. "Textual Analysis in Accounting and Finance: A Survey". *Journal of Accounting Research* 54 (4): 1187–1230. ISSN: 0021-8456. doi:10.1111/1475-679x.12123.

– . 2011. "When Is a Liability Not a Liability? Textual Analysis, Dictionaries, and 10-Ks". *The Journal of Finance* 66 (1): 35–65. ISSN: 1540-6261. doi:10.1111/j.1540-6261.2010.01625.x.

Mann, Janelle, and Peter Sephton. 2016. "Global relationships across crude oil benchmarks". *Journal of Commodity Markets* 2 (1): 1–5. ISSN: 2405-8513. doi:10.1016/j.jcomm.2016.04.002.

Mohammadi, Hassan, and Lixian Su. 2010. "International evidence on crude oil price dynamics: Applications of ARIMA-GARCH models". *Energy Economics* 32 (5): 1001–1008. ISSN: 0140-9883. doi:10.1016/j.eneco.2010.04.009.

Mudinas, Andrius, Dell Zhang, and Mark Levene. 2019. "Market Trend Prediction using Sentiment Analysis: Lessons Learned and Paths Forward". eprint: 1903.05440.

Pennington, Jeffrey, Richard Socher, and Christopher Manning. 2014. "Glove: Global Vectors for Word Representation". *Proceedings of the 2014 Conference on Empirical Methods in Natural Language Processing (EMNLP)*: 1532–1543. doi:10.3115/v1/d14-1162.

Roache, Shaun K, and Marco Rossi. 2010. "The effects of economic news on commodity prices". *The Quarterly Review of Economics and Finance* 50 (3): 377–385. ISSN: 1062-9769. doi:10.1016/j.qref.2010.02.007.

Smales, Lee A. 2014. "News sentiment in the gold futures market". *Journal of Banking & Finance* 49:275–286. ISSN: 0378-4266. doi:10.1016/j.jbankfin.2014.09.006.

Smirnov, Nikolai. 1939. "On the estimation of the discrepancy between empirical curves of distribution for two independent samples". *Bulletin Moscow University* 2:3–16.

Smola, Alex J., and Bernhard Schölkopf. 2004. "A tutorial on support vector regression". *Statistics and Computing* 14 (3): 199–222. ISSN: 0960-3174. doi:10.1023/b:stco.0000035301.49549.88.

Tetlock, Paul C. 2007. "Giving Content to Investor Sentiment: The Role of Media in the Stock Market". *The Journal of Finance* 62 (3): 1139–1168. ISSN: 0022-1082. doi:10.1111/j.1540-6261.2007.01232.x.

Timmermann, Allan, and Clive W J Granger. 2004. "Efficient market hypothesis and forecasting". *International Journal of Forecasting* 20 (1): 15–27. ISSN: 0169-2070. doi:10.1016/s0169-2070(03)00012-8.

Ushakov, Nikolai G. 1999. *Selected Topics in Characteristic Functions*. ISBN: 9783110935981.

7 Appendix

Figure 26:

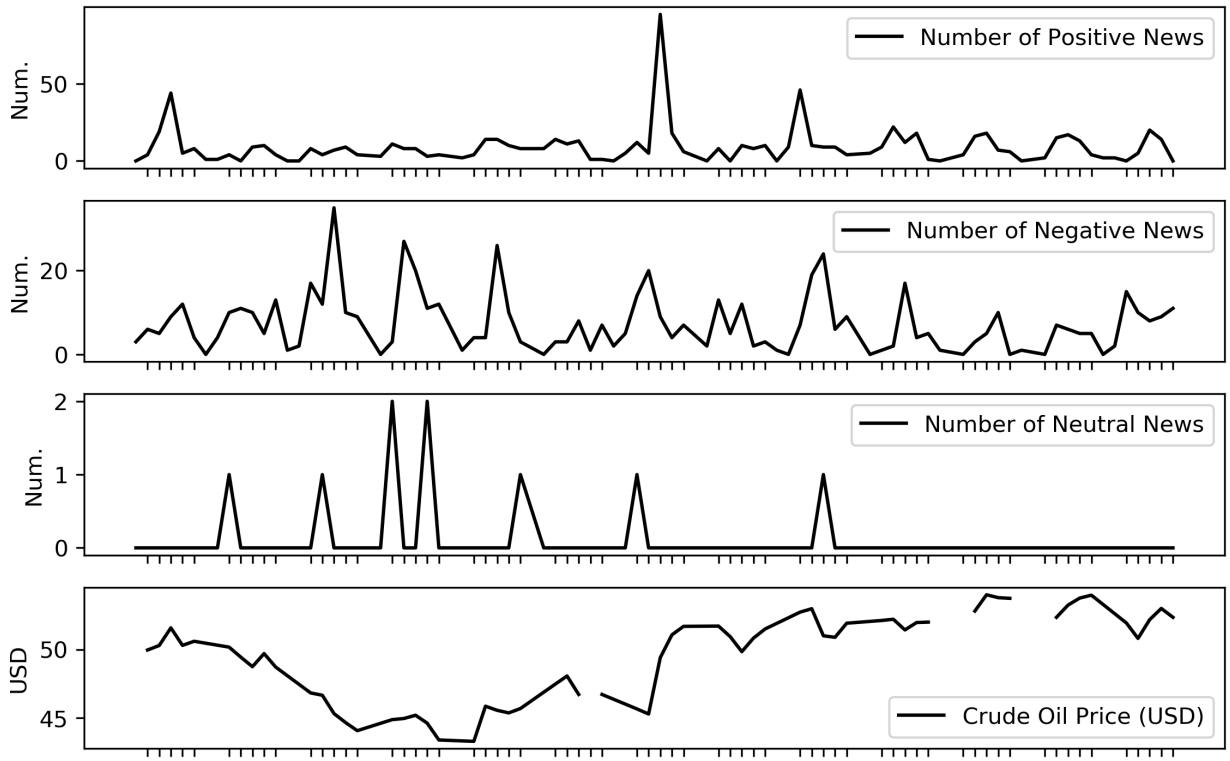

Figure 27:

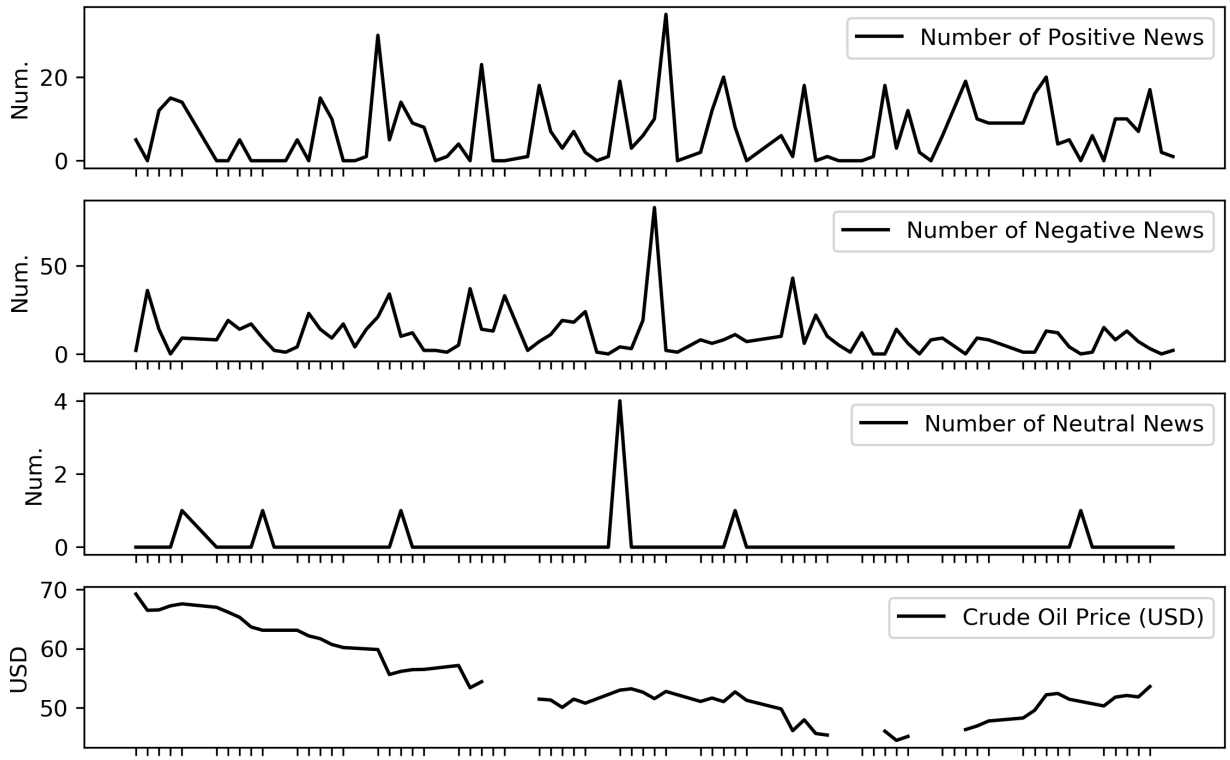
Number of Positive News
Num.
20
0
Number of Negative News
Num.
50
0
Number of Neutral News
Num.
4
2
0
Crude Oil Price (USD)
USD
70
60
50

Figure 28:

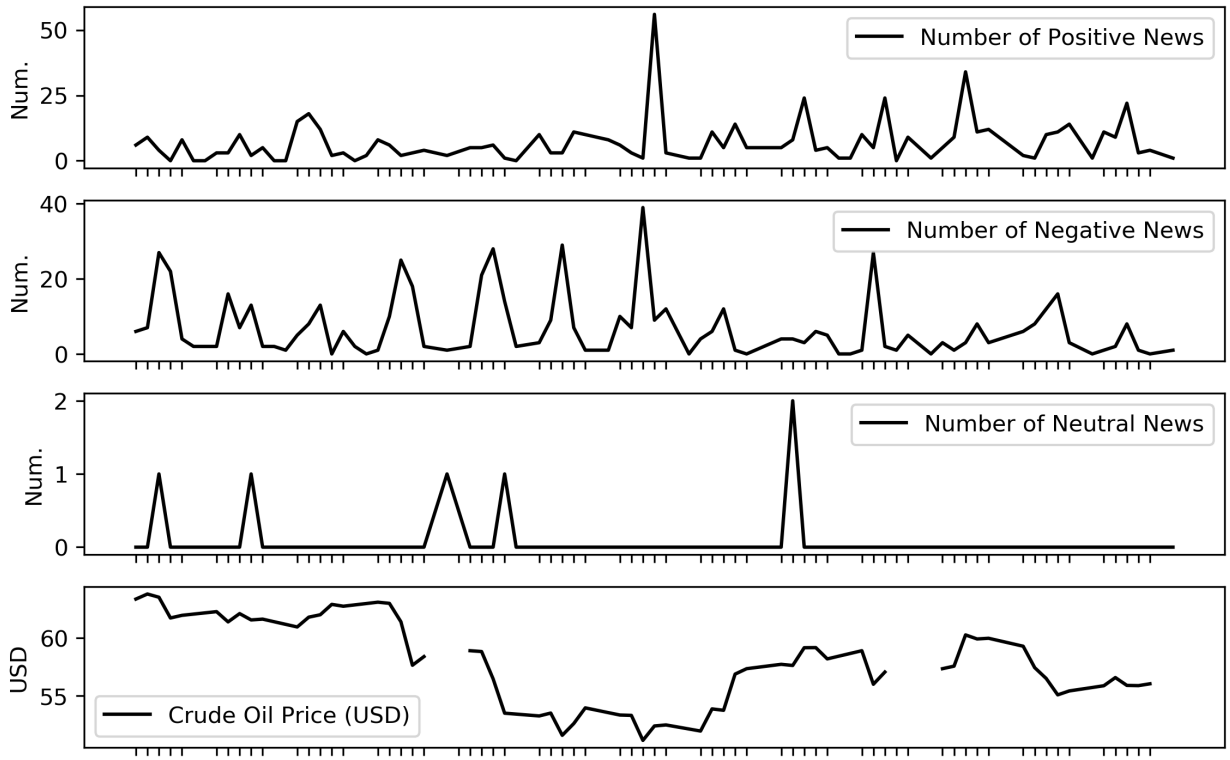
Number of Positive News
Num.
50
25
0
Number of Negative News
Num.
40
20
0
Number of Neutral News
Num.
2
1
0
Crude Oil Price (USD)
USD
60
55

Table 30: All Categories of Positive News

Category	Number of Positive news
commodity-price-gain	22,893
commodity-futures-gain	11,648
supply-decrease-commodity	5,845
imports-up	2,705
commodity-buy-target	1,171
demand-increase-commodity	1,070
exports-down	1,020
spill-commodity	787
commodity-offer-target	429
demand-guidance-increase-commodity	375
price-target-upgrade	332
exports-guidance-down	217
technical-view-bullish	193
supply-guidance-decrease-commodity	186
imports-guidance-up	122
relative-strength-index-oversold	85
embargo	80
piracy	57
pipeline-bombing-attack	32
force-majeure-commodity	26
tanker-accident-commodity	17
export-tax-guidance-decrease	11
pipeline-accident-commodity	11
platform-accident-commodity	11
import-tax-guidance-decrease	8
drilling-suspended-commodity	8
facility-close-output	6
import-tax-decrease	6
hijacking-target-commodity	4
export-tax-decrease	3
market-guidance-up-commodity	2
refinery-accident-commodity	2
facility-accident-commodity	2
technical-price-level-support-bullish	1
pipeline-bombing-threat	1

Table 31: All Categories of Negative News

Category	Number of negative news
commodity-price-loss	26,475
commodity-futures-loss	12,818
supply-increase-commodity	6,629
imports-down	2,017
exports-up	1,308
resource-discovery-commodity	1,179
technical-view-bearish	1,172
demand-decrease-commodity	650
demand-guidance-decrease-commodity	341
commodity-sell-target	303
supply-guidance-increase-commodity	268
price-target-downgrade	261
exports-guidance-up	208
technical-price-level-resistance-bearish	150
force-majeure-lifted-commodity	85
imports-guidance-down	75
export-tax-increase	29
drilling-commodity	27
export-tax-guidance-increase	24
facility-upgrade-output	21
import-tax-increase	18
relative-strength-index-overbought	16
embargo-lifted	12
import-tax-guidance-increase	9
facility-open-output	5
facility-accident-contained-commodity	4
import-tax	3
export-tax	3
facility-sale-output	3
hijacking-released-commodity	1
tax-break-ended	1

Table 32: Filtering using Event Sentiment Score

r	Num Negative	Num Neutral	Num Positive
0	50.59% (100.00%)	3.25% (100.00%)	46.15% (100.00%)
1	50.57% (99.96%)	3.29% (101.24%)	46.13% (99.96%)
2	50.55% (99.91%)	3.33% (102.33%)	46.12% (99.93%)
3	50.52% (99.85%)	3.39% (104.08%)	46.09% (99.87%)
4	50.51% (99.83%)	3.82% (117.33%)	45.68% (98.96%)
5	50.20% (99.23%)	5.24% (161.14%)	44.55% (96.54%)
6	50.04% (98.91%)	5.42% (166.77%)	44.54% (96.49%)
7	50.01% (98.85%)	5.47% (168.07%)	44.52% (96.46%)
8	49.99% (98.81%)	5.51% (169.27%)	44.50% (96.42%)
9	48.88% (96.62%)	6.82% (209.80%)	44.29% (95.97%)
10	48.84% (96.53%)	6.91% (212.45%)	44.25% (95.88%)
11	48.82% (96.49%)	6.97% (214.20%)	44.21% (95.80%)
12	48.78% (96.41%)	7.86% (241.51%)	43.37% (93.96%)
13	48.74% (96.33%)	7.92% (243.55%)	43.34% (93.90%)
14	48.72% (96.29%)	7.96% (244.64%)	43.33% (93.87%)
15	11.93% (23.58%)	44.76% (1376.20%)	43.31% (93.83%)
16	11.88% (23.49%)	44.83% (1378.41%)	43.28% (93.78%)
17	11.85% (23.42%)	44.89% (1379.97%)	43.27% (93.74%)
18	11.82% (23.37%)	77.24% (2374.59%)	10.94% (23.71%)
19	11.80% (23.33%)	77.27% (2375.51%)	10.93% (23.68%)
20	11.73% (23.18%)	77.41% (2379.79%)	10.87% (23.55%)
21	11.42% (22.57%)	77.82% (2392.47%)	10.76% (23.32%)
22	5.69% (11.25%)	83.65% (2571.83%)	10.66% (23.09%)
23	5.57% (11.00%)	83.86% (2578.38%)	10.57% (22.90%)
24	5.53% (10.94%)	89.23% (2743.37%)	5.24% (11.34%)
25	5.41% (10.70%)	89.43% (2749.47%)	5.16% (11.17%)
26	5.37% (10.62%)	89.52% (2752.20%)	5.11% (11.07%)
27	5.32% (10.51%)	89.65% (2756.25%)	5.03% (10.91%)
28	4.23% (8.37%)	91.79% (2822.05%)	3.98% (8.62%)
29	4.21% (8.33%)	91.86% (2824.12%)	3.93% (8.51%)
30	4.18% (8.27%)	91.90% (2825.38%)	3.92% (8.49%)

Table 33: Filtering using Weighted Event Sentiment Score

r	Num Negative	Num Neutral	Num Positive
1	46.54% (100.00%)	9.06% (100.00%)	44.40% (100.00%)
1	39.25% (84.33%)	20.32% (224.32%)	40.43% (91.06%)
2	33.69% (72.40%)	29.93% (330.42%)	36.37% (81.92%)
3	31.12% (66.87%)	34.62% (382.22%)	34.25% (77.14%)
4	28.35% (60.92%)	40.08% (442.46%)	31.57% (71.10%)
5	25.24% (54.24%)	46.49% (513.20%)	28.27% (63.66%)
6	24.92% (53.54%)	49.89% (550.79%)	25.19% (56.73%)
7	21.78% (46.79%)	53.19% (587.19%)	25.03% (56.38%)
8	21.42% (46.04%)	57.06% (629.93%)	21.51% (48.45%)
9	18.09% (38.87%)	60.76% (670.80%)	21.15% (47.62%)
10	17.51% (37.64%)	61.39% (677.67%)	21.10% (47.52%)
11	17.46% (37.53%)	65.26% (720.44%)	17.28% (38.91%)
12	14.07% (30.23%)	69.17% (763.62%)	16.76% (37.75%)
13	13.25% (28.47%)	70.03% (773.05%)	16.72% (37.66%)
14	13.15% (28.25%)	74.32% (820.49%)	12.53% (28.22%)
15	9.83% (21.13%)	77.68% (857.58%)	12.48% (28.11%)
16	9.66% (20.76%)	77.96% (860.57%)	12.38% (27.88%)
17	8.29% (17.82%)	79.37% (876.19%)	12.34% (27.79%)
18	8.18% (17.57%)	84.22% (929.75%)	7.60% (17.12%)
19	8.06% (17.31%)	84.49% (932.75%)	7.45% (16.78%)
20	7.98% (17.15%)	84.63% (934.20%)	7.39% (16.65%)
21	7.51% (16.14%)	85.37% (942.46%)	7.12% (16.03%)
22	4.77% (10.24%)	88.20% (973.67%)	7.03% (15.84%)
23	4.66% (10.01%)	88.42% (976.11%)	6.92% (15.58%)
24	4.48% (9.63%)	91.35% (1008.46%)	4.17% (9.39%)
25	4.22% (9.06%)	91.95% (1015.06%)	3.83% (8.63%)
26	4.16% (8.95%)	92.06% (1016.33%)	3.77% (8.50%)
27	4.09% (8.79%)	92.24% (1018.25%)	3.67% (8.27%)
28	3.28% (7.04%)	93.86% (1036.13%)	2.86% (6.45%)
29	2.95% (6.34%)	94.23% (1040.22%)	2.82% (6.35%)
30	2.92% (6.27%)	94.31% (1041.09%)	2.77% (6.25%)

Table 34: News on Bloomberg June 12, 2019

PALM OIL: Futures Drop to 6-Month Low as Crude Oil Prices Slump
OIL DAYBOOK AMERICAS: Saudis Sell Extra Crude to China; EIA Data
Oil Stocks Fall Most in Europe as Rising Stockpiles Hit Crude
Oil Extends Slide After EIA Reports Surprise U.S. Crude Inventory Increase
U.S. DOE Crude Oil Inventories, Production and Imports (Table)
Canadian Stocks Fall After Crude Oil Plunges as Storage Swells
OIL DAYBOOK ASIA: Oil Demand Shrivels Amid U.S.-China Trade War
DJ News Highlights: Top Energy News of the Day
Enterprise Sees U.S. Oil Exports Topping Saudi Arabia's by 2025
Market Realist: Commodities Are Mixed Early on June 18
China Times Crude Purchases Well During Oil-Price Slump
TOPLive Starts: Analysis of the EIA Crude Oil Inventory Report
Malaysia May Palm Oil Stockpiles -10.3% M/m to 2.45M Tons
RTT News: Crude Oil Futures Plunge Sharply, Settle At 5-month Low
Oil Plunges as U.S. Storage Swells, Demand Outlook Worsens
Copper and Crude Oil 'Do-or-Die' Elevate Macroeconomic Risks
Malaysia May Crude Palm Oil Prices -3.6% M/m at MYR1,947/Ton
German Baltic Port Boosts Crude Imports to Offset Druzhba Loss
Energy Stocks Teeter Along With Oil After Inventory Build
Oil Holds Near Lows on U.S. Stockpile Build, Poor Demand Outlook
Saudis Heed China Request for More Oil as Supplies Squeezed
OIL BRIEF: OPEC Makes First Nod to Curbs in 2020
Action Forex: Crude Oil: Oil Trading Lower, Ahead Of EIA's Weekly Crude Oil Stockpiles Data
Oil & Gas 360: Crude Oil Inventories Up 2.2 Million Barrels
Watch Oil Stocks as Higher Inventories, Trade Jitters Hit Crude
WTI Crude Oil Is Teetering on the Cliff's Edge
Crude oil futures fall on weak global cues
UNIAN: Reuters: Oil falls 1% on weaker oil demand growth, surprise gain in U.S. crude stocks
Times Now: Crude oil prices down more than 2% on US inventories, demand worries
Xinhua: Oil prices decline on increasing U.S. crude inventories
Crude Oil WTI (F) Has Changed Elliott Wave Count
Crude Oil Brent Has Changed Elliott Wave Count
ASIA CRUDE: Chinese Buyer Gets Extra Saudi Oil; Iran July OSPs
World Oil Inventory Days Above 10-Year Average
Crude Oil Capitulation on Tap
HoustonChronicle: Nation's crude oil supplies jump again as oil prices slip further
S. Korea's Hyundai Oilbank Cuts Oil Processing Rate by About 3%
Bonds Gain as Crude Price Slides Ahead of CPI Data: Inside India
*CRUDE OIL INVENTORIES ROSE 2.21 MLN BARRELS, EIA SAYS
Oil's 2019 Weakness Has Roots in 2018's Strength: Liam Denning
EIA Stockpile Hits 20-Month High Amid Subdued Demand: Lee
OIL MKT DRIVERS: API Reports Build; OPEC Latest; Demand Worries
OIL DAYBOOK EUROPE: OPEC+ 'Very Close' on Cuts Extension; EIA
Bus Day Nigeria: OPEC crude oil output shrinks in May, organisation struggles to avoid $40 oil
[Delayed] J.P. Morgan 2019 Energy Equity Conference: The Question Bank
Saudi Arabia Economic Report - 2019 - English
[Delayed] MLP 1Q19 PM Handbook: Earnings Defies Fears with Operating Leverage & Optimization on Display; Much Needed Signs of
Halyk Finance Daily (ENG) - June 12, 2019
Sunwah Kingsway - Willas-Array (854 HK)
BOBCAPS First Light | Monthly Eco Chartbook, Inflation and IIP

Table 35: News on Bloomberg June 13, 2019

✓Market Realist: US Crude Oil Near $50: Why Denbury Resources Might Be in Trouble
✓Oil-Services Benchmark Rebounds Along With U.S. Crude: Chart
Watch Oil Stocks as Brent Surges After Report of Tanker on Fire
✓WTI Crude Oil $80 Resistance, Then $70, Now $60 Suggests a Trend
PALM OIL: Futures Rally From 6-Month Low as Crude Oil, Soy Jumps
Oil is surging after a suspected torpedo attack on 2 tankers in the Gulf of Oman
Oil Slump Forces Norwegian Producer OKEA to Slash IPO Price
Oil Stocks Rise Following Jump in Crude After Tankers Attacked
✓OPEC May Crude Oil Production in OPEC Countries (Table)
AP NewsAlert: Benchmark Brent Crude Oil Rises 4% in Trading to Over $62 a Barrel After Oil Tanker Incident in Gulf of Oman
Oil Prices Spike As Navy Rushes To New Attack But OPEC Flashes This Warning
Staring at a Recessionary Abyss, Crude Oil Needs an OPEC+ Jolt
DJ Energy Calendar - 2019 Futures, Options Dates - Jun 13
Oil Stocks Climb With Crude After Tanker Attack: EU Energy Wrap
DJ Oil Jumps After Tanker Attacks in Middle East -- 2nd Update
RUBBER: Futures Reverse Losses in Singapore as Crude Oil Jumps
DJ News Highlights: Top Energy News of the Day
U.S. Stocks Climb With Treasuries; Crude Oil Jumps: Markets Wrap
✓OPEC Allies May Need to Deepen, Extend Crude Oil Supply Cuts
✓OIL BRIEF: Crude Surges as Gulf Tankers Suffer New Attack
Cartagena Oil Refinery Crude Unit Restarted, Spain's Repsol Says
Bus Day Nigeria: Crude oil build up sends price lower
Hormuz Attacks May Raise Oil's Premium Despite Risk of Slowdown
India Infoline: Energy Preview: Crude Melts 3.50% On MCX
RTT News: Oil Futures Settle Sharply Higher After Attacks On Oil Tankers
Europe Stocks Recover From Earlier Losses as Oil Shares Advance
Times Now: Crude oil slumps 4% on US crude build, slowing demand fears
URGENT: The Latest: Crude Over $62 a Barrel After Mideast Incident
Oil Surges on Mideast Tanker Incident, Stocks Rise
Tanker Attacks Are Threatening the World's Most Important Oil Route
How Tanker Attacks on a Skinny Waterway Could Affect Oil Prices
Tanker Attack in Gulf of Oman Sends Oil Price Soaring
Xinhua: U.S. oil imports, exports down last week: EIA
HoustonChronicle: Crude-oil marketing and transportation firm rides rising tide of oil prices
Investing.com: Oil Prices Recover Slightly After Plunging 4% on Crude Inventories Data
Market Realist: Why Diamondback Energy Has Been an Outperformer This Quarter
DJ ICE Gas Oil/Brent Crude Oil/WTI Open Interest - Jun 13
Persian Gulf Remains Bedrock for VLCC Loadings
$40 WTI Crude Is More Likely Than $60
Action Forex: Crude Oil: Oil Trading Lower In The Asian Session
DJ ICE Brent Crude Oil Volume - Jun 13
Oil Jumps From Near Five-Month Low After Report Tanker on Fire
COMMODITIES
Crude Prices Rebound From Five-month Low as Tanker Attack Fuels Fears Over Key Oil Artery
DBH: Nigeria earns $236bn from petroleum exports in five years
Too much supply uncertainty; new highs point to 465, 472 3/4 soon - HIGHTOWER
[Delayed] Iron ore: Upgrading Chinese steel demand and iron ore prices, but the peak disruption is likely behind us
FW: LatAm Daily